2024

The role of UCHL1 in skeletal muscle development and regeneration

Ryan Antony

THE ROLE OF UCHL1 IN SKELETAL MUSCLE DEVELOPMENT AND REGENERATION

By

Ryan Antony

B.S., Florida Institute of Technology, 2019

A Thesis Submitted in Partial Fulfillment of
the Requirements for the Degree of Master of Science

Division of Basic Biomedical Sciences

Sanford School of Medicine
In the Graduate School
The University of South Dakota
May 2024

The members of the Committee appointed to examine
the Thesis of Ryan Antony
find it satisfactory and recommend that it be accepted.

DocuSigned by:
Yifan Li
AE32C7B4EBBE406...
Chairperson

DocuSigned by:
Hong Zheng
A669B3E3E65348D...

DocuSigned by:
Khosrow Pezvani
55F3B8D0E065450...

Abstract

Ubiquitin C-terminal hydrolase L1 (UCHL1) is a deubiquitinating enzyme that was originally discovered in neurons. UCHL1 is also expressed in skeletal muscle, but its functions remain to be fully understood. Myogenesis is a critical process involved in embryonic development, growth, and regeneration following injury. Skeletal muscle injury is prevalent in trauma and surgical procedures, and skeletal muscle ischemia-reperfusion (IR) injury is a common yet dangerous public health problem. Here we reported that UCHL1 negatively affects muscle growth during aging as well as the regeneration process following IR injury. First, we observed that UCHL1 knockdown in C2C12 myoblasts resulted in increased myotube width and differentiation. Furthermore, UCHL1 KD consistently upregulated myogenin and MyoD protein levels, key proteins involved in myogenesis, at multiple time points throughout myotube differentiation. Consistent with this *in vitro* result, skeletal muscle specific knockout (smKO) of UCHL1 increased muscle fiber diameter in both 1- and 2-month-old mice. Interestingly, smKO of UCHL1 caused muscle-dependent fiber type switching and myosin heavy chain expression. Following skeletal muscle IR injury, myogenin and MyoD protein expression was upregulated in injured muscle from smKO mice. In addition to this, KO mice also had increased muscle function and performance after injury compared to control mice when subjected to *in situ* contractile testing. UCHL1 smKO also exhibit a decreased inflammatory response following injury, as well as upregulation of proteins associated with mitophagy. As a novel finding, we also found that UCHL1 regulates p62 expression and release via deubiquitinating function. This data suggests that skeletal muscle UCHL1 may function as a negative regulator of myogenesis, both during growth, and repair following injury.

Thesis Advisor: 

Dr. Yifan Li

Acknowledgements

First and foremost, I want to thank Dr. Yifan Li for everything throughout my tenure as both a research associate and graduate student. I have been given countless opportunities to learn and gain experience from that I may not have received had I been under a different mentor, for which I will always be grateful. Though our time in the lab has come to a somewhat sudden end, my 5 years in the lab working with you has shown me how truly passionate someone can be towards research, and towards the betterment of their students. My experience has been nothing but the utmost pleasure, and I would not be where I am without your help and guidance, Dr. Li.

I wish to express my sincere gratitude to my graduate advisory committee, Dr. Hong Zheng, and Dr. Khosrow Rezvani. I am extremely appreciative of your support, encouragement, comments, and suggestions. I want to further extend my thanks to Dr. Rezvani for the opportunity to collaborate on your research as an additional author on multiple publications, as well as my appreciation for your guidance and mentorship.

I want to also thank Katherine and Morgan for their help in the lab and their friendship throughout our time in the lab together. Morgan, I could not have made the transition from research associate to grad student without your help making gels and genotyping. Katherine, thank you for your help with experiments, guidance as a fellow student, and for your friendship. As you demonstrate your devotion to anything you do, you have made me want to follow in your footsteps and strive for nothing less than excellence.

Additionally, I would like to extend my thank you to Jessie Freeling for her willingness to listen to our (grad students) problems and grievances. Thank you for always being willing to open your door and provide guidance, and your friendship as well.

Lastly, I am grateful for my family and their support of my continued training and education. Living away from home does not come without its hardships, and I would not have made it through without you.

Table of Contents

List of Tables

List of Figures

CHAPTER 1

Background and significance

1.1 Overview

Skeletal muscle accounts for roughly 40% of mass within the human body, containing 50-70% of all body proteins, and is responsible for functions such as posture and locomotion, thermogenesis, metabolism, and energy homeostasis[22-24]. Myogenesis, the formation of muscle tissue, is a critical mechanism for development of the musculoskeletal system, maintenance of healthy adult muscle cells, and regeneration of damaged muscle following injury[27,31-33]. UCHL1 was originally discovered as a deubiquitinating enzyme in neuronal tissue, accounting for 1-2% of total soluble protein in the brain. Though the function of UCHL1 in the nervous system has been well documented, its semi-recent discovery in skeletal muscle has opened the door to other possibilities. Despite previous studies highlighting the involvement of UCHL1 in skeletal muscle growth, its role in skeletal muscle development and regeneration are not completely understood.

This thesis will highlight the functions and mechanisms of UCHL1 in skeletal muscle development and regeneration.

1.2 Literature review

1.2.1. UCHL1

Ubiquitin Carboxyl-terminal Hydrolase L1 (UCHL1) was originally discovered as a brain specific protein, accounting for approximately 5-10% of cytoplasmic protein in neuronal cells[1]. UCHL1, along with Bap1, UCHL3, and UCHL5, belong to the UCH class of deubiquitinating enzymes (DUBs) which are primarily responsible for removing monoubiquitin or polyubiquitin chains from substrates[2,3]. The post-translational modification of substrates by attaching or detaching ubiquitin or ubiquitin chains is a key regulatory mechanism for numerous processes including cell growth and protein degradation via the ubiquitin-proteosome system (UPS)[3-5]. It has been found that, at least in neurons, UCHL1 is not only responsible for removing ubiquitin from specific proteins, but also for maintaining a pool of free monoubiquitin[2,6]. Interestingly, UCHL1 has been shown to have a dual function of both adding and removing ubiquitin from protein substrates, setting it apart from other DUBs[2]. Pathologically, UCHL1 has been associated with neurodegenerative disorders such as Alzheimer's disease and Parkinson's disease where decreased levels of UCHL1 are linked to impaired protein degradation[1,2,6]. Beyond the nervous system, UCHL1 has been found to be expressed in other organs such as the pancreas, liver, spleen, skeletal muscle, as well as playing a role in cancer[7-9]. In cancers within various tissue types, studies have shown that UCHL1 promotes cancer cell proliferation and metastasis[10-13]; however, other studies have shown that UCHL1 acts as a tumor suppressor[14-16], supporting the notion that UCHL1 has many functional mechanisms throughout the body that remain unclear. Previous studies from our lab have highlighted the expression of UCHL1 in skeletal muscle, associating it with muscular function and myogenic activities[17-21]. Despite the findings, the role of UCHL1 in skeletal muscle functions remains to be fully understood.

1.2.2. Skeletal Muscle

Skeletal muscle makes up approximately 40% of body mass and contains roughly 50-70% of all body proteins[22]. Aside from being responsible for locomotion and maintaining posture, skeletal muscle significantly contributes to functions such as metabolism, thermogenesis, and

energy homeostasis[22-24]. Skeletal muscle consists of muscle fibers/myofibers which are elongated, multinucleated cells which are surrounded by a plasma membrane known as the sarcolemma, then surrounded by the basal lamina, a layer of extracellular matrix (ECM)[25]. Within the myofibers themselves are actin and myosin filaments, and upon a change in intracellular calcium ion gradients, the filaments will interact, and contraction will occur[29,30]. The myosin protein exists as groupings of subunits, those subunits being myosin heavy chain (MYH) and myosin light chain (MYL)[80]. The function of MYH is to provide energy needed for contraction via ATPase activity, whereas despite the vast diversity, the function of MYL is to provide structural integrity, as well as regulation of certain functions[80,81]. The nuclei of myofibers, also known as

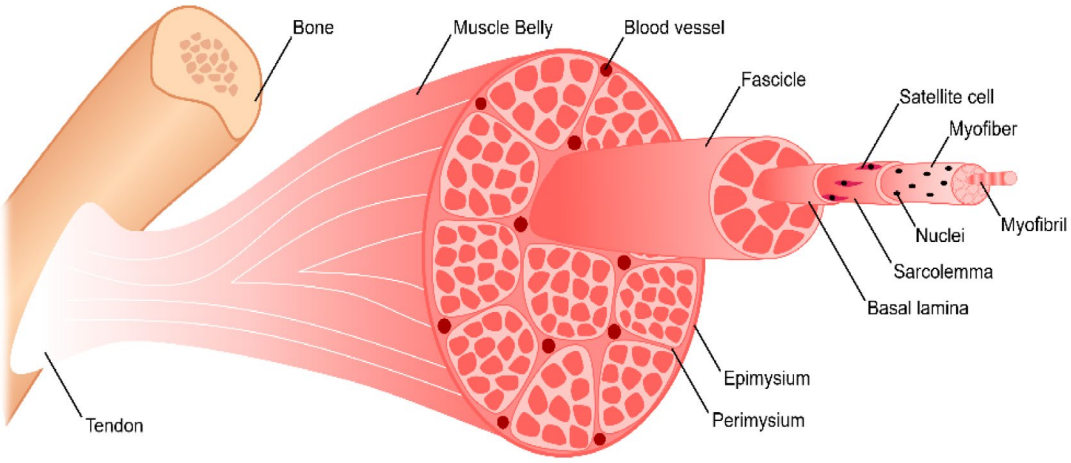

Figure 1: Anatomy of Skeletal Muscle. Carnes, M. E., & Pins, G. D. (2020). Skeletal muscle tissue engineering: biomaterials-based strategies for the treatment of volumetric muscle loss. Bioengineering, 7(3), 85.

myonuclei, are peripherally located along the myofiber and are responsible for physiologic processes. In addition to myonuclei, muscle satellite cells are dispersed along the myofiber, remaining in an unactive, quiescent state until such time occurs, such as injury, where activation will cause the satellite cells to proliferate and differentiate into mature myofibers[25-27]; this process is commonly referred to as myogenesis and will be elaborated on in the next section.

The myofibers themselves can be divided into three different types of fiber based on contractile properties and physiologic features; these are also known as type 1, type 2a, and type 2b muscle fibers. Type 1 fibers are referred to as “slow twitch” fibers due to their nature of slow contraction and resistance to fatiguing. Type 1 muscle fibers rely on oxidative metabolism for energy and are rich in mitochondria. Type 2 fibers are referred to as “fast twitch” muscle fibers due to their fast contractile nature and are easily fatigued compared to type 1 fibers. Type 2b muscle fibers are comparably opposite to type 1 fibers having less mitochondria and relying on glycolytic metabolism for energy. Type 2a fibers can be seen as an intermediate between type 1 and type 2b, having a mix of oxidative and glycolytic myofibers which results in fast contraction and moderate fatiguing; this fiber type also has a concentration of mitochondria between what would be found in type 1 and type 2b[25,28]. Similar to other organs and tissues, skeletal muscle must maintain and replenish healthy cells, and much like other organs, skeletal muscle can become damaged and must be repaired. Both of the aforementioned processes rely on myogenesis[27].

1.2.3. Myogenesis

The generation of muscle, also known as myogenesis, is necessary for the development of skeletal muscle during embryonic growth as well as for maintenance of healthy adult skeletal muscle, thus can be divided into the two distinct phases[27,31-33]. During embryonic development, skeletal muscle fibers are generated from mesoderm-derived structures with additional fibers being added along the “template fibers”[31]. These additional fibers originate as myogenic progenitor cells, cells expressing Pax3 and Pax7, transcription factors of myogenic regulatory genes, before undergoing significant proliferation and migration, ultimately differentiating into embryonic muscle fibers upon induction of transcription factors known as myogenic regulatory factors (MRFs)[33,34]. Similar to embryonic muscle development, regeneration of adult muscle relies on the proliferation and differentiation of myogenic precursors; however, unlike embryonic development, adult muscle myogenesis is driven by the activation of already present quiescent stem cells which migrate to the site of injury at the basal lamina, or to adjacent myofibers if the basal lamina is destroyed[33,35].

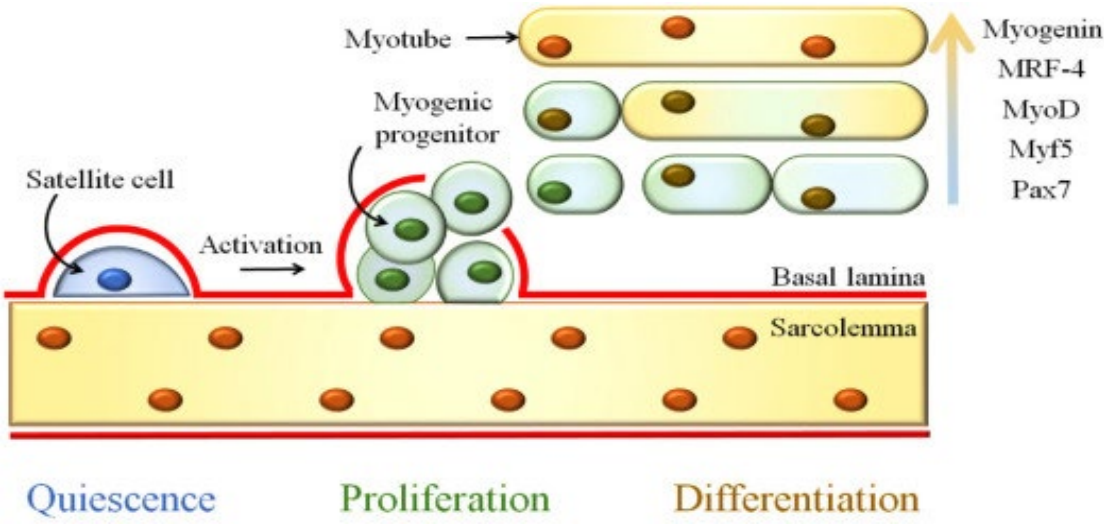

Figure 2: Myogenesis in adult muscle**.** Arrighi, N. (2018). Definition and classification of stem cells. Stem Cells, 2018, 1-45.

Both of these myogenic processes are dependent on the expression of MRFs which direct the precursors through proliferation, differentiation, and maturation into mature muscle fibers. The 4 MRFs, Myf-5, MyoD, myogenin, and MRF4, play specific roles in signaling of myogenesis and are expressed at differing times and durations[31-33]. Notably, Myf-5 and MyoD control genes related to cell proliferation whereas myogenin and MRF4 are associated with genes responsible for cell differentiation; however, combined activity of MRFs during stages of myogenesis gives rise to the expression of other MRFs and depends heavily on the stage of the cell cycle[34,36,37]. During embryonic development, sonic hedgehog (Shh) signaling activity induced expression of Myf-5, followed by expression of MyoD as a result of Wnt signaling. Myogenin and MRF4 then becomes expressed and fluctuates through several wave of differentiation beginning with embryonic myoblasts and ending with muscle satellite cells[33,36,37]. Myogenic regulatory factors function almost identically in adult myogenesis with Myf-5 and MyoD being expressed first, followed by myogenin and MRF4 until the satellite cells form mature muscle fibers[33,36,37]. As mentioned previously, myogenesis in adult muscle serves two functions, to maintain healthy muscle cells, and to regenerate muscle cells following injury.

1.2.4. Ischemia-Reperfusion Injury

Skeletal muscle injuries, often sports-related, can be sustained by various causes such as directly via trauma, or indirectly by ischemia or neurological disorders[38]. Ischemia describes the condition in which blood flow is restricted to an area of the body, and this is commonly followed by reperfusion, the return of sufficient blood flow to the previously restricted area; this is known as ischemia-reperfusion (IR) injury and is a common injury to the heart and brain as it is associated with stroke, myocardial infarction, and peripheral vascular disease, among other conditions[39-42]. In addition to the heart and brain, IR injury is the most common type of skeletal muscle injury and is often a result of surgical procedures, specifically those that utilize tourniquet application[39,40,43,44]. Given the nature of IR injury, tissue damage varies based on how long the ischemic period lasts. Studies have shown that muscle is somewhat tolerant to ischemia for up to 4 hours while nerve changes are reversible for up to 8 hours, and less sensitive tissue types tolerant for longer[39]. Despite the variation in damage, even short term ischemia will induce a hypoxic environment, leading to cell dysfunction and death as a result of altered ion exchange/transport[41]. Although one might assume that the return of blood flow would be nothing but beneficial, reperfusion brings more cellular damage. When the restriction to blood flow is removed, the innate and adaptive immune responses become active, triggering neutrophil infiltration and cell death programs[39,46]. Additionally, the production of reactive oxygen species (ROS) during reperfusion causes damage to the cell membrane via lipid peroxidation[40], and an overload of calcium to muscle cells causes contracture[45]. Although treatments of IR injury are being extensively researched, there are currently no established means of injury reduction or regenerative therapies[47-50].

1.2.5. The Inflammatory Response

Inflammation occurs as an essential and protective response as a means to ensure survival during tissue injury and infection[51-53]. The inflammatory response is in place to remove harmful stimuli from the body such as foreign pathogens and other dangerous molecules, as well as regulating the healing of damaged tissue[51]. In addition to the classical roles that inflammation

plays, published studies highlight the importance of inflammation in cellular homeostasis, both in the quality control of homeostatic maintenance, as well as restoring homeostasis after injury[53]. However similar, not all inflammatory responses in the body are the same. Inflammation can exist as an acute response, a chronic condition, low grade, and can occur sterilely[51-53]. Sterile inflammation can occur as a result of chronic diseases, but it can also occur acutely as a result of sterile injury such as ischemia-reperfusion[54,55]. Although inflammation is usually beneficial to the body, it can act as a double-edged sword by causing more damage whether it be infection-driven or sterile. In the case of sterile inflammation, dead cells and their released intracellular contents including RNA, DNA, ATP, and enzymes, are all harmful stimuli capable of inducing inflammation. Regardless of sterility or not, the acute inflammatory response on a basic level behaves the same. Upon injury or infection, blood delivers leukocytes to the response site, often recruited by innate immune system receptors recognizing the signal, and this recognition is mediated by mast cells and tissue resident macrophages[52]. Following skeletal muscle injury, such as IR injury, infiltrating neutrophils drive the inflammatory response initially, followed by infiltration of monocytes and macrophages. Macrophages exert proinflammatory action at the early stage of inflammation, but undergo a phenotypic shift to promote inflammation resolution and myogenesis, proving crucial in the regeneration of skeletal muscle[56-59]. In inflammation and injury, autophagy plays a critical protective role in the resolution of cellular damage[60-62].

1.2.6. Mitophagy

Autophagy, characterized by orchestrated processes of the autophagosome-lysosome system, is a cellular process responsible for the removal of denatured proteins, damaged organelles, and foreign pathogens via lysosomal degradation[60]. Under normal conditions, autophagy is restricted by mammalian target of rapamycin (mTOR), and upon conditions such as oxidative stress, reduction of glucose and amino acids, or other environmental changes, mTOR function will become inhibited, triggering a signaling cascade which induces autophagosome formation[60-65]. Autophagy also plays a role in initiating the immune response following infection or tissue damage[65]. In addition to removal of pathogens and misfolded proteins, autophagy also

promotes cell surface antigen presentation, prevents necrosis, promotes cellular senescence, and protects against genome instability[66]. Due to the large abundance of proteins in skeletal muscle, the coordination and regulation of the UPS and autophagosome-lysosome systems must be strictly controlled as excessive degradation can result in muscular atrophy and dysfunctional metabolism and energy homeostasis[67,68]. It is well known that mitochondria play a key role in energy metabolism and homeostasis[69-72]. As mitochondria are complex organelles, it has been found that they also significantly contribute to the control of stress responses, being able to release ROS and apoptotic factors[71]. Mitochondrial health is critical for cellular processes; unhealthy, damaged, and aged mitochondria must be removed efficiently. Autophagy is responsible for the selective removal and disposal of the unhealthy organelles, and this process is known as mitophagy[73]. It has been shown that mitophagy is regulated by PTEN-induced putative kinase protein 1 (PINK1) and parkin, and similar to UCHL1, mutations of these genes have been linked to neurological diseases such as Parkinson's disease[73-76].

Goals and hypothesis of this study

The overarching goal of this study is to understand the role and underlying mechanism of skeletal muscle UCHL1 in muscle development and regeneration after injury. We hypothesize that UCHL1 is a negative regulator during muscle development and regeneration.

CHAPTER 2

Materials and Methods

2.1 In Vitro Cell Culture

2.1.1 C2C12 cell line

C2C12 mouse myoblasts (American Type Culture Collection) were seeded and cultured in complete media which consisted of HyClone high glucose Dulbecco's Modified Eagle's Medium (DMEM, Cytiva) containing 10% FBS, 1% penicillin/streptomycin (P/S), and 1% HEPES solution and incubated until 90% confluent. Upon 90% confluency, medium was removed and replaced with differentiating medium which consisted of DMEM supplemented with 2% horse serum, 1% P/S, and 1% HEPES. Medium was changed every 48 hours until cells had reached the desired stage of differentiation prior to treatment.

2.1.2 UCHL1 gene knockdown

Upon 90% confluency in CM, cells were transfected in incomplete medium (ICM) (DMEM with no additives), lipofectamine RNAiMAX transfection reagent (Invitrogen), and either control or UCHL1 siRNA. 400 µL of ICM was mixed with 24 µL of transfection reagent. 200 µL of ICM was mixed with 12 µL of control or UCHL1 siRNA, and then mixed with 200 µL of the reagent mixture. The siRNA/reagent mixture was let to incubate at room temperature for 10 minutes while medium in the 35 mm dishes was removed and replaced with 1 mL of ICM. After 10 minutes, 100 µL of the appropriate mixture was added to each dish, giving an equal number of dishes containing control or UCHL1 siRNA. The dishes were incubated for 6-8 hours before adding 1 mL of DM. After 12 more hours of incubation medium was then removed and changed to 2 mL of DM, and cells were allowed to differentiate for 1-6 days before being collected and homegenized for western blot.

2.1.3 UCHL1 gene overexpression

For UCHL1 overexpression, cells were treated with adenovirus (Ad) expressing GFP, WT UCHL1, or C90S mutant UCHL1. 1 µL of adenovirus expressing GFP, which acted as the control, was mixed with 5 µL of ICM to give a 6 fold dilution. 1 µL of WT or C90S UCHL1 were mixed with 3 µL of ICM to give a 4 fold dilution. After cells achieved 90% confluency in CM, medium was removed and replaced with 1 mL of ICM. 1 µL of the appropriate diluted adenovirus mixture was added to 35 mm dishes,

giving an equal number of control and UCHL1 overexpression dishes. Cells were returned to the incubator for 6-8 hours before adding 1 mL of DM. After another 12 hours of incubation, medium was removed and replaced with 2 mL of DM, being changed every 24 hours until being collected after 72 hours in DM.

2.1.4 Hydrogen peroxide treatment

To induce oxidative stress in C2C12 cells, hydrogen peroxide (H2O2) treatment was used following the previously published method[79]. 35% aqueous H2O2 was diluted to a concentration of 200 mM in ICM. Cells that had already been differentiating for 72 hours had the medium removed and replaced with 2 mL of fresh DM. 5 µL of the diluted H2O2 was added to dishes, giving a final concentration of 500 µM. Cells were then returned to the incubator for 12 hours of treatment prior to collecting and homogenizing for western blot.

2.1.5 Recombinant P62 treatment

Upon 90% cell confluency in CM, medium was removed and replaced with 2 mL of DM supplemented with recombinant P62 at a concentration of 50 or 100ng/mL; both DM and rP62 were changed every 48 hours until cell collection on the 6th day in DM/rP62.

2.2 Animal Study

2.2.1 Ethical animal use and welfare

The animal use in this study were approved by the University of South Dakota IACUC (protocol number 01-05-22-25D) and was in compliance with NIH guidelines.

2.2.2 UCHL1 skeletal muscle specific knockout mice

The UCHL1 skeletal muscle specific knockout mouse model has been previously described[20]. The mouse strain “UCHL1 HEPD0603_7_h04” was generated from EUCOMM/KOMP-CSD ES cells and provided by Medical Research Council (MRC) on behalf of the European Mouse Mutant Archive (EMMA). This mouse strain was crossed with mice expressing Flp recombinase to remove the targeting cassette (LacZ and Neo genes). Offspring of the UCHL1-Flp recombinase mice were then bred with wild type (WT) mice to remove the Flp transgene; this new strain carried the exon 2 floxed UCHL1 gene and was free of Flp. The floxed UCHL1 mice were bred with mice expressing Cre

recombinase driven by the myosin light chain 1 promotor (Myl1$^{tm1(cre)sjb}$/J, Jackson lab #024713) to generate a UCHL1 skeletal muscle-specific knockout (smKO) mouse strain. PCR and appropriate primers for UCHL1 and My1 Cre were used to ensure specific genotyping.

2.2.3 Non-invasive model of hindlimb Ischemia-reperfusion injury

Adapted from the published method[77] with modification, three-month-old male and female UCHL1 smKO and control mice were anesthetized using isoflurane inhalant (2-3%). Buprenorphine SR was administered at a concentration of 1mg/kg to control pain after waking. An orthodontic rubber band (ORB) was placed at hip level on the right hind limb using a McGivney ligator applicator, leaving the left hind limb as the contralateral control. The rubber band was left in place for 90 minutes; complete ischemia was confirmed using laser Doppler imaging (Moor Instruments). Following the period of ischemia, the ORB was removed allowing reperfusion for 3-12 days. Animals were sacrificed and tissue was collected from the IR injured and contralateral control limbs.

2.2.4 *In situ* muscle contraction

In situ muscle contraction was also done as previously described[78] with modification. In brief, mice were anesthetized using a mixture of Urethane (2mg/kg) and α-chloralose (50mg/kg) via intraperitoneal injection. The skin of the right hindlimb was removed. The gastrocnemius-plantaris muscle complex was isolated and connected to a force transducer, and a pair of electrodes were placed at the proximal and distal ends of the gastrocnemius-plantaris complex. The muscle complex contractile function was tested with several stimuli including various preload, frequency, and voltage settings. The procedure was then repeated for the contralateral hindlimb which serves as the control for this experiment.

2.2.5 Tissue collection

Mice were anesthetized using Urethane alpha chloralose via intraperitoneal injection as described above prior to euthanasia. Mice were euthanized via decapitation for total blood collection. After carefully removing the skin of the hindlimb, soleus and extensor digitorum longus (EDL) were collected from each hindlimb for western blot. Tibialis anterior (TA) muscles were coated in OCT and

snap frozen in dry prechilled 2-methylbutane. The frozen TA muscles were then prepared in blocks of OCT for cryo-sectioning and stored at -80ºC until used for histology/immunofluorescent staining. Lastly, the plantaris muscle from each hindlimb was collected for QPCR.

2.3 Sample Preparation and Assays

2.3.1 Western blot

For western blot using cells, cells medium was removed from dishes and 1 mL of DM was added. Cells were scraped using a plastic scraper until completely detached from dishes. PBS containing cells was then pipetted up and down several times in the dish before transferring to a 1.5 mL DNA/RNA free tube with snap cap. Tubes were centrifuged for 10 minutes at 10,000 RPM and PBS was then removed. Lysis buffer was created by mixing 1X radioimmunoprecipitation assay (RIPA) buffer (RPI, R26200) with protease inhibitor cocktail 3 (RPI, P50700) and phosphatase inhibitor cocktail 2 (Thermofisher, J61022-AA) at a ratio of 100:1:1. 60 µL of lysis buffer was added to tubes containing cell pellets. Tubes were then placed in a bullet blender (Next Advance) and shaken for 5 minutes followed by 15 minutes of sitting; this was repeated two more times before briefly spinning the tubes down. 20 µL of pre-warmed beta-mercaptoethanol loading buffer was added to tubes before vortexing and spinning down again. Tubes were heated at 90ºC for 15 minutes, vortexed, and centrifuged for 5 minutes at 10,000 RPM before storing until use.

For western blot using tissue samples, tissue collected previously in 1.5 mL DNA/RNA free tubes was briefly homogenized using a plastic pestle. 200 µL of lysis buffer (same as above) was added to tubes and homogenized again using the pestles with a drill. Samples were left to sit in lysis buffer for 30 minutes prior to a last round of homogenization. Pestles were removed and tubes were centrifuged for 10 minutes at 10,000 RPM. Protein concentration of the supernatant was then measured and normalized using a BCA assay. 90 µL of supernatant was added into new tubes, along with 30 µL of pre-warmed loading buffer. Tubes were vortexed and spun down before heating at 90ºC for 15 minutes, then vortexed and spun down again prior to freezing until use.

15 µL of tissue protein sample, or 20 µL of cell protein sample, was pipetted into 10-15% gradient gels and fractionated under 100 V for approximately 3 hours. Proteins were transferred onto a 0.22

μm nitrocellulose membrane (Santa Cruz, SC3718) using a trans-blot apparatus (Bio-Rad) at 350 mV for 2 hours. Proteins were fixed onto membranes in 50% methanol for 30 minutes at 4ºC, then 30 minutes at 37ºC. Membranes were then incubated at room temperature in 3% milk for 1 hour. Proteins were detected using primary antibodies diluted in PBST, incubated overnight at 4ºC on a rocker. Membranes were washed 3 times in PBST for 5 minutes each, then incubated in appropriate secondary antibodies conjugated with Alexa-680 or Alexa-800 and diluted in PBST for 1 hour at room temperature. Membranes were washed twice in PBST for 5 minutes each, followed by 5 minutes in PBS. Proteins were visualized via scanning on a LI-COR scanner (LI-COR biosciences) and the signal was quantified using LI-COR Image Studio 5.2 software. Primar and secondary antibodies are shown in **Table #1**.

Table 1: Antibodies used in study

Primary Antibodies						
Antibody	**Brand**	**Catalog Number**	**Molecular Weight (kDa)**	**Source**	**WB Dilution**	**IHC Dilution**
Actin	Santa Cruz	47778	45	Ms	1:1000	1:500
AKT	Cell Signaling	9272S	60	Rb	1:1000	
BAD5	DSHB	BA-D5-S	222	Ms	1:50	1:100
BFF3	DSHB	BF-F3-S	223	Ms	1:50	1:100
CD11b (488)	BioLegend	101254	170	Ms		1:250
CD68 (594)	BioLegend	137020	85-115	Ms		1:250
DRP1	Cell Signaling	8570S	78-82	Rb	1:1000	
Dystrophin	Abcam	15277	440	Rb		1:200
eMYHC	DSHB	F1.652-S	200	Ms	1:50	
GAPDH	Santa Cruz	166574	37	Ms	1:1000	
MYH (1/2/4/6)	Santa Cruz	32732	200	Ms	1:500	
MyoD	Santa Cruz	377460	45	Ms	1:500	
Myogenin	Santa Cruz	52903	34	Ms	1:500	
nMYHC	DSHB	N3.36-S	200	Ms	1:50	
Parkin	BioLegend	808501	42	Ms	1:500	
P-AKT (S473)	Cell Signaling	4051S	60	Ms	1:1000	
P-Pink1 (S228)	Cell Signaling	89010S	75	Rb	1:1000	
P-4EBP1 (T37/46)	Cell Signaling	2855S	15	Rb	1:1000	
P62	Cell Signaling	D1Q5S	62	Rb	1:1000	
SC71	DSHB	SC-71-S	222	Ms	1:50	1:100
SOD2	Cell Signaling	D3X8F	22	Rb	1:1000	
UCHL1	Protein Tech	14730-1-AP	25	Rb	1:1000	

Table 1: Antibodies used in study

Secondary Antibodies					
Antibody	**Brand**	**Catalog Number**	**Source**	**WB Dilution**	**IHC Dilution**
AlexaFluor Plus 800 IgG	Invitrogen	A32730	Goat anti-mouse	1:10000	
AlexaFluor 680 IgG	Invitrogen	A21109	Goat anti-rabbit	1:10000	
AlexaFluor 488 IgM	Invitrogen	A21042	Goat anti-mouse		1:500
AlexaFluor 488 IgG	Invitrogen	A11008	Goat anti-rabbit		1:500
AlexaFluor 594 IgG	Invitrogen	A11032	Goat anti-mouse		1:500
AlexaFluor 594 IgG	Invitrogen	A11012	Goat anti-rabbit		1:500

2.3.2 Immunoprecipitation (IP) assay

C2C12 cells were seeded into 70mm dishes in CM and incubated until 90% confluent. Medium was removed and 3 mL of ICM was added to each dish. Cells were then infected with Ad-UCHL1-HA virus using 2 µL of the dilution listed above. After 5-6 hours of incubation, 3 mL of DM was added to each dish and returned to the incubator. After 12 hours of incubation, medium was removed and 5 mL of DM was added to each dish. DM was changed every 24 hours until cells were harvested at the 72 hour mark.

After 72 hours in DM, medium was removed from dishes and 1 mL of ice-cold PBS was added. Cells were scraped and the suspension was transferred to a pre-chilled 1.5 mL DNA/RNA free tube. Tubes were then centrifuged at 5,000 RPM for 5 minutes. During centrifugation, IP lysis buffer was made by mixing 20mM Tris-HCL (pH 8.0), 137 mM NaCl, 1% NP-40, 2mM EDTA. The cell pellet was resuspended in 300 µL of IP lysis buffer mixed with 3 µL protease inhibitor cocktail 3. Tubes were then rotated on a rotor for 2 hours at 4ºC followed by centrifugation at 10,000 RPM for 10 minutes. Cell lysate supernatant was transferred to a new tube and the pellet was discarded.

20 µL of lysate supernatant was added to a 1.5 mL tube along with 3 µL of the appropriate antibody (1 µg/µL), then rotated for 120-150 minutes at 4ºC. While tubes were rotating, agarose beads were prepared. In a 1.5 mL tube, 80 µL of bead slurry was added and then washed 3 times with cold PBS for 5 minutes each. Tubes were centrifuged at 150 RPM for 5 minutes and PBS was discarded. Beads were resuspended in 40 µL of IP lysis buffer. The lysate/antibody mixture was then added to the agarose bead suspension and final volume was adjusted to 500 mL with cold PBS. Samples were placed on rotator and left to rotate overnight at 4ºC. Tubes were spun down at 150 RPM for 5 minutes and the supernatant was transferred to another tube. IP wash buffer was created by mixing 10 mM Tris (pH 7.4), 1 mM EDTA, 1 mM EGTA (pH 8.0), 150 mM NaCl, and 1% Triton X-100. The bead-protein-antibody complex was washed in 1 mL of IP wash buffer and then spun down at 150 RPM and buffer was discarded; this process was repeated another 2 times. After removing the wash buffer from the third wash, 50 µL of 2X loading buffer was added to the bead complex. In a new tube, 20 µL of supernatant was mixed with 20 µL of 4X loading buffer to create the input sample.

Additionally, IP controls were created using agarose bead lysis buffer and antibody only, and agarose bead and lysate only, both mixed with an equal part 4X loading buffer. The tubes were then heated at 100ºC for 5 minutes, vortexed, and briefly spun down. Samples were ran using the above western blot method on a 10% gel, making sure to not load agarose beads with the sample supernatant.

2.3.3 Quantitative polymerase chain reaction (QPCR)

RNA preparation utilized the Direct-zol RNA microprep protocol and kit from Zymo research (Catalog #R2060-R2063). 400 µL of RNAzol was added to DNase/RNase free tubes containing plantaris muscle samples which were then homogenized using pestles. Tubes were centrifuged for 30 seconds at 15000 RPM, then the supernatant was transferred to new tubes with 400 µL of 100% ethanol. The supernatant and ethanol were thoroughly mixed prior to transferring to filter columns in new tubes. The tubes were again centrifuged for 30 seconds at 15000 RPM, or until the solution had completely passed through the filter column. Filter columns were transferred to new tubes at which point 400 µL of DirectZol prewash was added to the filter columns and spun down for 30 seconds at 15000 RPM; this step was repeated once. Prewash was removed from the tube and 700 µL of DirectZol wash buffer was added to the filter column and centrifuged for 1 minute at 15000 RPM or until completely filtered through. The empty filter columns were transferred to new 1.5ml tubes, then 20 µL of RNase free water was added to the columns before 1 minute of centrifugation at 15000 RPM or until completely filtered. The filter columns were discarded, and samples were normalized using nucleic acid concentrations obtained using a nanodrop spectrophotometer (Thermo nanodrop 2000). 10 µL of normalized sample was then combined with an equal amount of cDNA reverse transcriptase master mix (Thermo Catalog #4368814) and subjected to a reverse transcription program on the Eppendorf master cycler. 1 µL of cDNA was then mixed with 10 µL of taq (PowerUp SYBR green master mix, Catalog #A25742), 2 µL of RNase free water, and 2 µL of primer (IDT 18s, IDT Myogenin). Sample mixtures were then subjected to thermal cycling using the Applied Biosystems Step One Plus.

2.3.4 Hematoxylin and Eosin tissue staining

The H&E protocol used in this study is based off of the published H&E protocol[38]. Frozen slides/sections were taken from -80 degree storage and directly immersed into Meyers hematoxylin

for 10 minutes at room temperature. Slides were then placed under running tap water until the water was clear. Following this, slides were then immersed in 1% Eosin at room temperature for 3 minutes, then rinsed under tap water until clear. Lastly, slides were dehydrated with 70% ethanol for 20 seconds, 95% for 20 seconds, and 100% ethanol for 1 minute, followed by clearing in xylene for 3 minutes prior to mounting. The slides were examined using a Nikon microscope equipped with an Olympus DP73 camera.

2.3.5 Immunofluorescent staining

Frozen slides/sections were incubated in PBST at room temperature for 10 minutes prior to primary antibody incubation. Primary antibodies were diluted to 1:100 in PBS containing 5% BSA; slides were incubated overnight in 4º Celsius. Following incubation, slides were washed in PBS 3 times for 5 minutes each, then incubated with secondary antibody (1:500 dilution in PBS) for 1 hour at room temperature. Slides were then washed again 3 times in PBS for 5 minutes each, then mounted using Fluoromount mounting solution. The slides were imaged using a fluorescent Nikon microscope equipped with an Olympus DP73 camera. Primary and secondary antibodies used are shown in **Table 1**.

2.3.6 Enzyme-linked immunosorbent assay (ELISA)

The following method uses the protocol and reagents from the PathScan Total SQSTM1/p62 Sandwich ELISA kit (7814C, Cell Signaling). Prior to sample collection, reagents and wells were brought to room temperature. Cell media or blood serum samples were collected as previously mentioned. Samples were added to appropriate wells (50 µL for serum, 100µL for media) and an equal amount of detection antibody was then added. The wells were sealed and the plate was placed on a shaker at 400 rpm for 1 hour at room temperature. Samples were discarded and wells were washed 4 times with 200 µL of 1X wash buffer per well, striking a paper towel between washes to ensure all wash buffer was removed. 100 µL of TMB substrate was added to each well and wells were sealed prior to the plate being covered with tin foil and left to incubate at room temperature for

15 minutes on a shaker at 400 rpm. 100 µL of STOP solution was then added to each well and the absorbance was read using an Infinite M200 plate reader (Tecan) and Magellan software.

2.4 Data Analysis

Data are presented as mean ± standard deviation (SD). One-way ANOVA followed by Tukey's post hoc test or student's t test were applied using GraphPad Prism software. Differences were considered statistically significant at $p<0.05$. Significant differences were denoted by *=$p<0.05$, **=$p<0.005$, ***=$p<0.0005$, ****=$p<0.00005$.

CHAPTER 3

Specific Aim #1 Results

Specific Aim #1: To further characterize the function of UCHL1 during skeletal muscle development.

3.1 UCHL1 knockdown increases myoblast differentiation and myotube formation

To confirm the findings previously published regarding the association between UCHL1 and myoblast differentiation, UCHL1 was knocked down in C2C12 myoblasts using siRNA, and cells were allowed to differentiate for up to 5 days. As expected, we observed significantly larger myotube widths at both days 3 and 5 of differentiation in cells treated with UCHL1 siRNA when compared to cells treated with control siRNA (Fig.3).

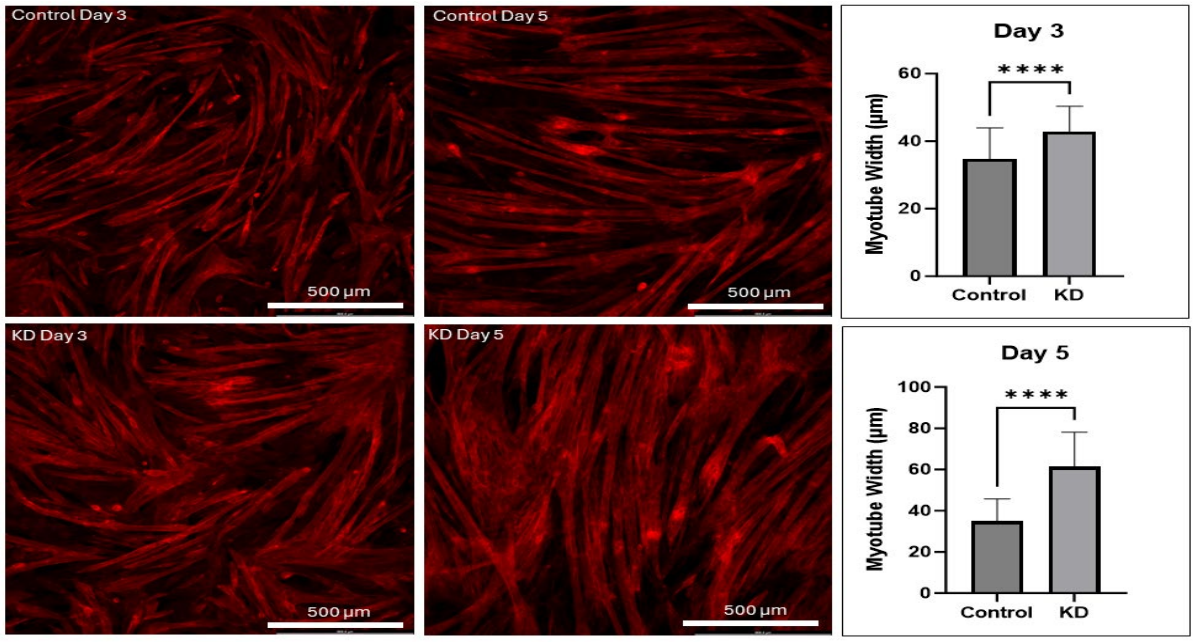

Figure 3: Knockdown of UCHL1 promotes myotube differentiation. Representative beta-actin immunofluorescent images and myotube width quantification between control (top) and UCHL1 knockdown (bottom) from day 3 (left) and day 5 (right).

The increase of myotube size when UCHL1 is knocked down supports that UCHL1 is a negative regulator of myoblast differentiation.

3.2 Manipulation of UCHL1 upregulates myogenic factors

Given the upregulated myotube differentiation due to UCHL1 knockdown, we further assessed how UCHL1 affects cell growth by analyzing myogenic proteins in UCHL1 knockdown cells. Western blot showed that basal levels of UCHL1 protein gradually decreased over the course of myoblast differentiation, whereas MyoD and myogenin, key proteins involved with myogenesis, gradually increased (Fig 4.A), which further supports that UCHL1 is inversely correlated with these myogenic proteins.

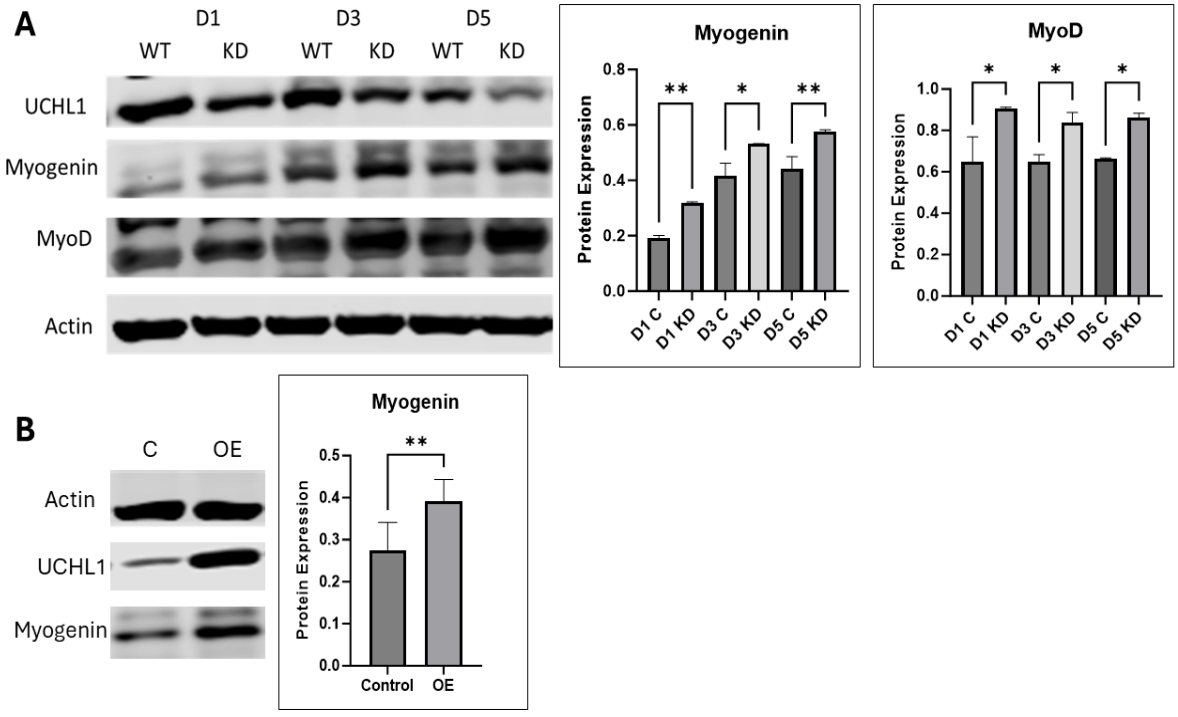

Figure 4: Manipulation of UCHL1 upregulates myogenic factors. **A:** Raw images and quantification of western blots for UCHL1, myogenin, MyoD, and beta-actin in control and UCHL1 knockdown cells after 1, 3, and 5 days of differentiation; **B:** Raw images and quantification of western blots for beta-actin, UCHL1, and myogenin in control and WT UCHL1 overexpressed cells after 3 days of differentiation; *P<0.05, n=2 35mm dishes at each time point.

Furthermore, when UCHL1 was knocked down, both myogenin and MyoD are significantly increased across all time points throughout differentiation when compared to control cells.

This data again supports the notion that UCHL1 is a negative regulator of myoblast differentiation. Interestingly, when WT UCHL1 is overexpressed, myogenin protein levels are still significantly increased when compared to control cells (Fig 4.B). The cause of this response is not clear at this time. Since the UCHL1 enzymatic activity was not measured in this study, it is not known whether the overexpressed

UCHL1 is functional. It is possible that overexpressed UCHL1 lacks deubiquitinating activity and thus causes a dominant negative effect similar to knockdown.

3.3 UCHL1 knockdown does not affect myosin heavy chain expression

After analyzing myogenic factors, we wanted to look at myosin heavy chain (MyHC), the contractile protein of muscle fibrils and a critical component of skeletal muscle function. UCHL1 was knocked down in C2C12 myoblasts and the cells were allowed to differentiate for up to 5 days. Western blot for total myosin heavy chain (1/2/4/6), embryonic myosin heavy chain, and neonatal myosin heavy chain showed the relative timeline for MyHC isoform expression in differentiating control and knockdown myotubes (Fig 5).

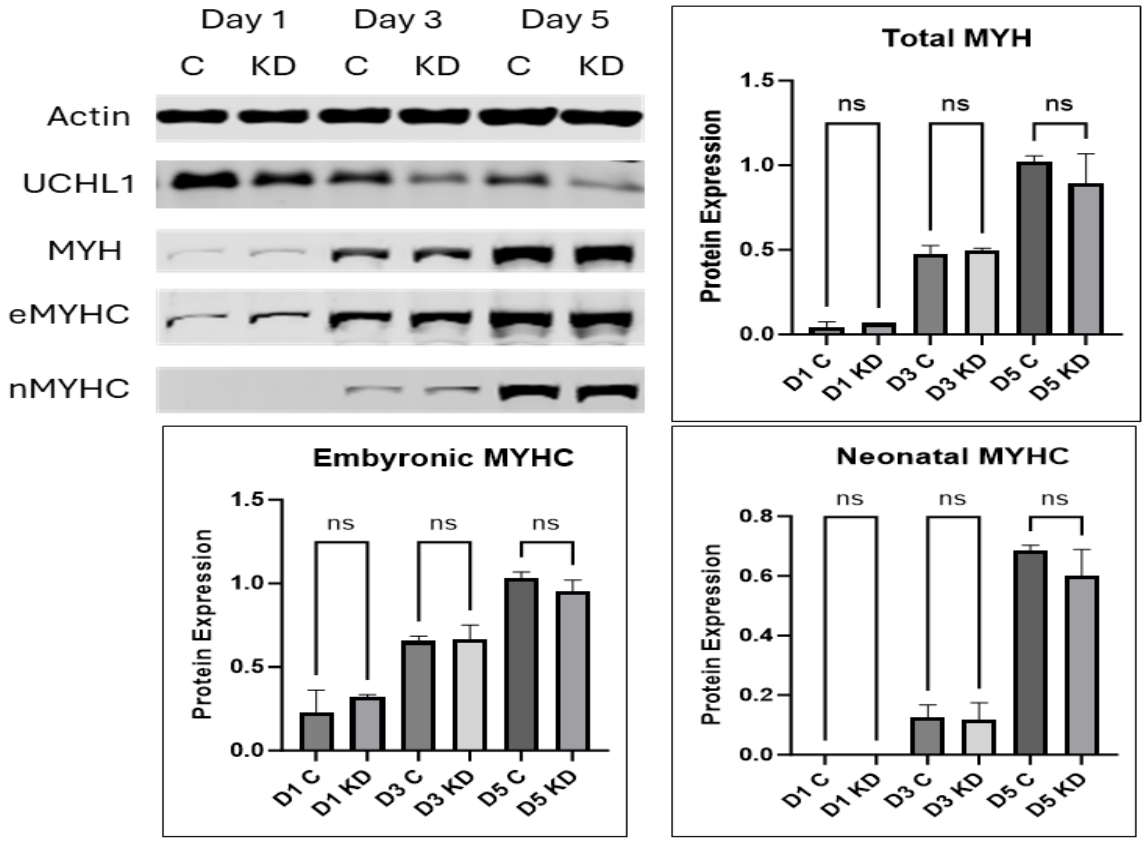

Figure 5: Myosin heavy chain is not affected by UCHL1 in vitro. Raw images and quantification of western blots for beta-actin, UCHL1, myosin heavy chain 1/2/4/6 (top right), embryonic myosin heavy chain (bottom left), and neonatal myosin heavy chain (bottom right); *P<0.05, n=2 dishes per time point.

Interestingly, knockdown of UCHL1 had no affect on embryonic, neonatal, and pan MyHC protein

expression despite UCHL1 KD cells exhibiting increased differentiation and myogenic factors. The antibody for pan MyHC recognizes several different MyHC isoforms. At this time, it is not clear whether any specific MyHC isoforms would be affected by UCHL1 KD, which should be further characterized in future studies.

3.4 UCHL1 skeletal muscle knockout increases fiber size

Given the upregulated differentiation of myoblasts as a result of UCHL1 knockdown *in vitro*, we assessed how UCHL1 affects muscle growth *in vivo* by measuring muscle fiber cross sectional area using our UCHL1 skeletal muscle specific knockout (smKO) mice.

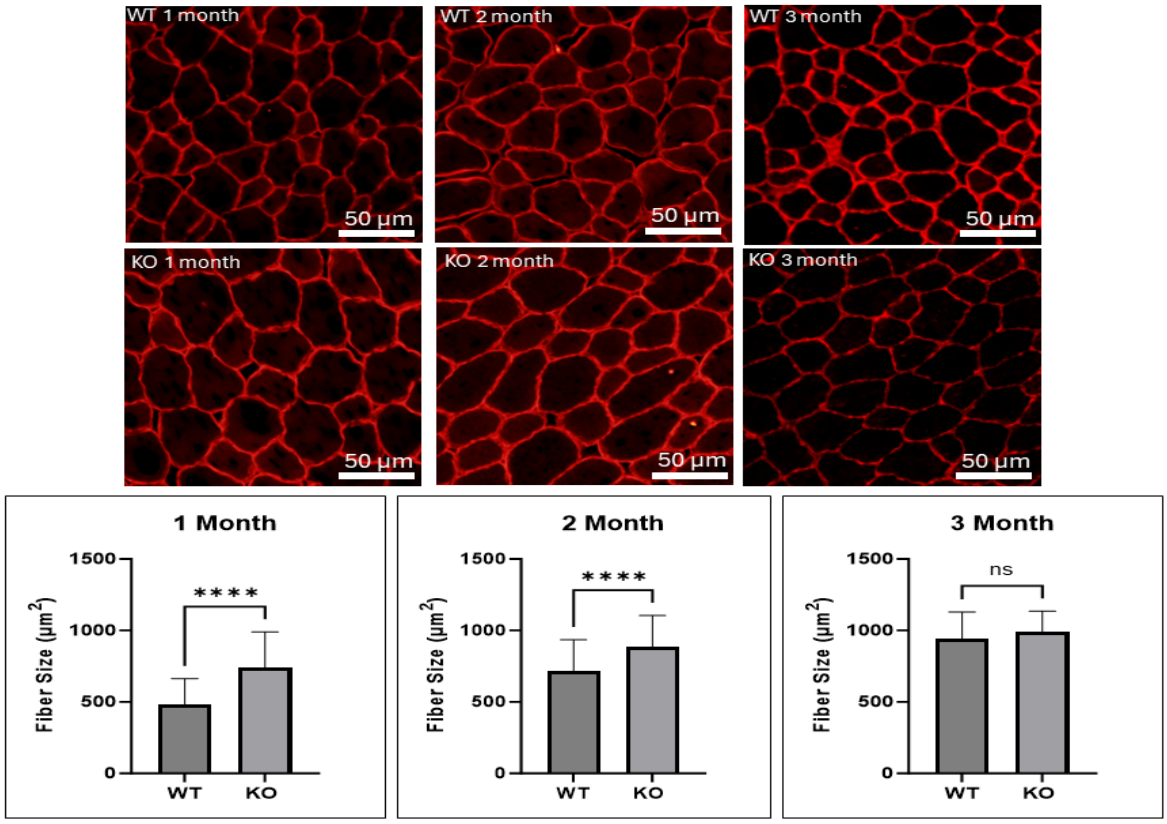

Figure 6: UCHL1 smKO increases muscle fiber size. Dystrophin immunofluorescent images and quantification between TA muscle sections from WT (top) and UCHL1 smKO (bottom) mice at 1 month(left), 2 month(middle), and 3 month(right) timepoints, *P<0.05, n=60 fibers.

Compared to the flox control mice, UCHL1 smKO mice exhibited significantly increased muscle fiber size (μm^2) at 1 and 2 months, but not at 3 months of age (Fig. 6), suggesting that UCHL1 had an inhibitory effect on muscle fiber development during earlier stages of muscle maturation.

3.5 Muscle fiber type is altered by UCHL1 knockout

Although the pan myosin heavy chain expression in C2C12 myotubes *in* vitro was unaffected by UCHL1 knockdown, we wanted to test whether any MyHC isoforms would

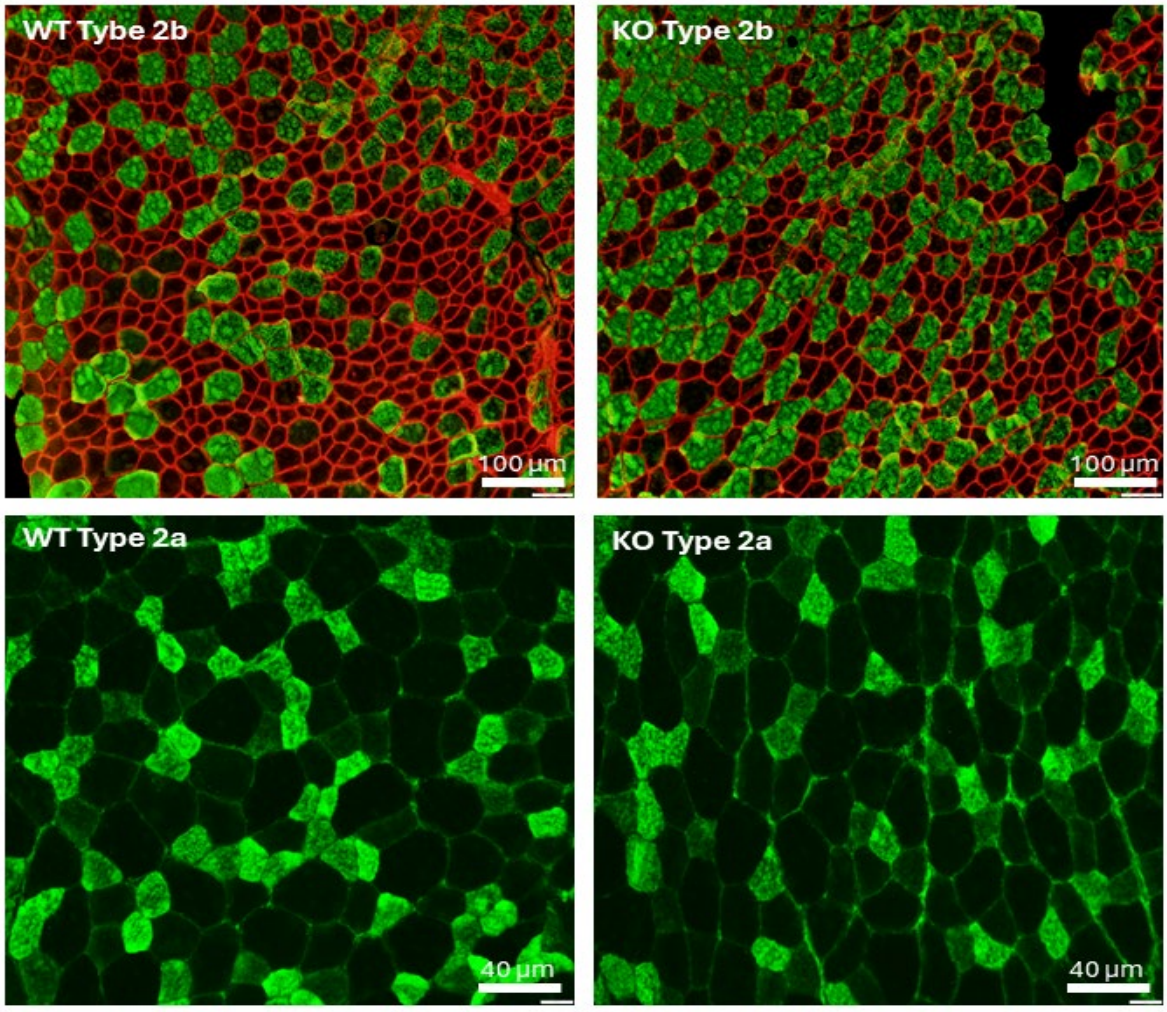

Figure 7: UCHL1 affects type 2 fiber concentration. Images of immunofluorescent staining between TA muscle sections using dystrophin (red) and BFF3 (green, top) for type 2b muscle fibers, and SC71 (green, bottom) for type 2a muscle fibers in WT (left) and UCHL1 smKO (right) mice.

be affected by UCHL1 smKO. Staining with fiber type specific antibodies showed that 3-month-old UCHL1 smKO mice exhibited increased Type-2b muscle fibers when compared to their WT counterparts (Fig 7, top). Type 2a fibers (Fig 7, bottom) were seen to have a slight decrease in number when comparing UCHL1 smKO mice to WT mice. Western blot (Fig 8, left) showed that UCHL1 smKO mice had increased myosin heavy chain in soleus, but significantly decreased myosin heavy chain in EDL (Fig 8, middle).

Additionally, UCHL1 smKO mice had significantly increased type 1 fiber expression in 3 month old soleus muscle, and significantly decreased type 1 fiber expression in 1 and 3 month old EDL muscle when compared to WT mice (Fig 8, right). This data suggests that UCHL1 plays a role in the regulation of fiber type specificity and myosin heavy chain during development *in vivo*.

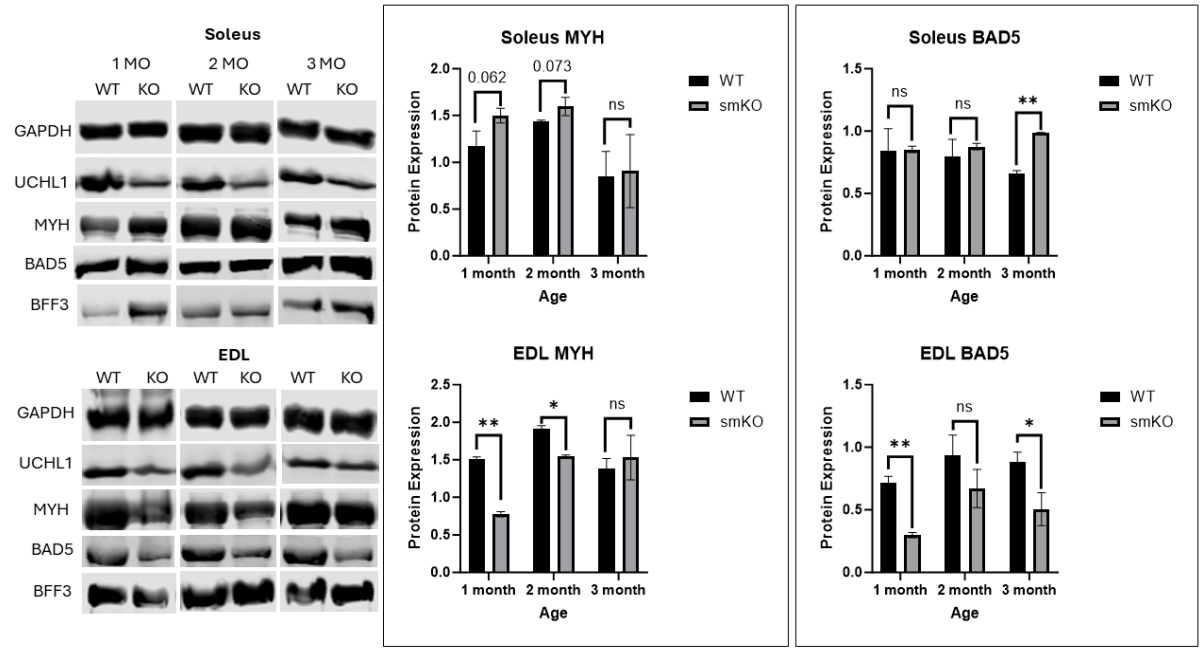

Figure 8: UCHL1 alters fiber type specificity. Raw images and quantification of western blots for GAPDH, UCHL1, MYH 1/2/4/6 (left), BAD5 (Type 1 fibers)(right), and BFF3 (Type 2b fibers) from soleus and EDL of WT and UCHL1 smKO mice; *P<0.05, n=2 mice per time point per genotype.

CHAPTER 4

Specific Aim #2 Results

Specific Aim #2: To investigate how UCHL1 affects regeneration following skeletal muscle injury

4.1 Model of hindlimb ischemia reperfusion injury

To study the role of UCHL1 in muscle injury and recovery, we developed a model of non-invasive hindlimb ischemia-reperfusion (IR) injury based on a previously published study[77]. During Ischemia, there was complete restriction of blood flow (Fig 9.A). Using H&E staining, and immunofluorescent staining with an antibody for CD68, a proinflammatory macrophage marker, the results showed that IR caused severe tissue damage at day 1 and 3, the majority of pro-inflammatory macrophage infiltration occurs around 3 days of reperfusion, whereas the muscle itself does not exhibit visible regeneration until 7 days after reperfusion (Fig 9.B and 9.C). Further, *in situ* contractile testing displayed that muscle had greater functional performance recovery at 12 days after injury when compared to muscle at 6 days after injury (Fig 9.D and 9.E)

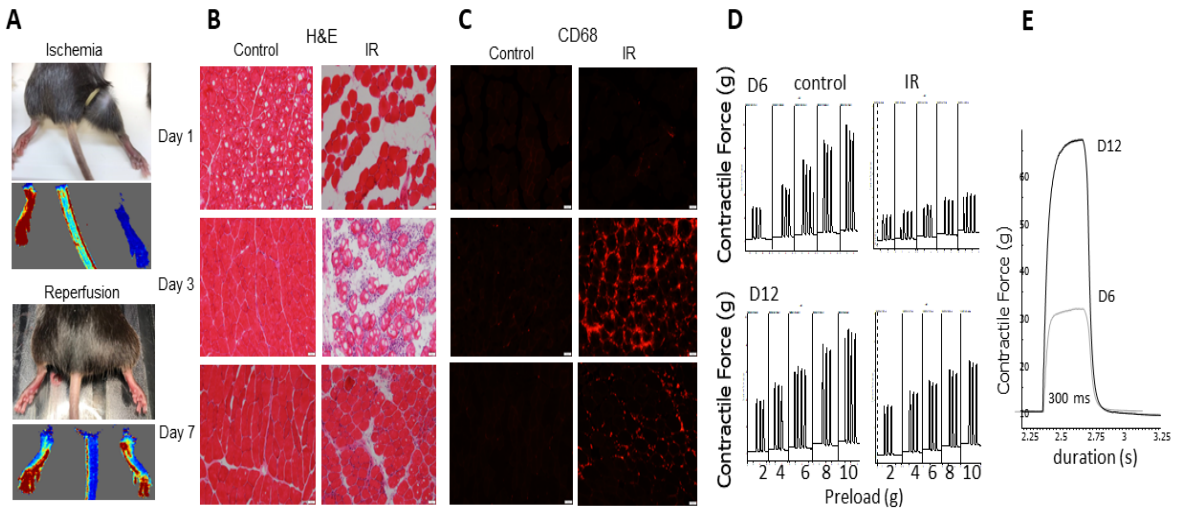

Figure 9: Non-invasive hindlimb ischemia-reperfusion injury model. **A:** Live (top of set) and laser doppler (bottom of set) images during ischemia (top) and reperfusion (bottom); **B:** H&E staining images of TA muscle sections from control limb (left) and IR limb (right) at days 1 (top), 3 (middle) and 7 (bottom); **C:** CD68 immunofluorescent images of TA muscle sections from control limb (left) and IR limb (right) at days 1 (top), 3 (middle), and 7 (bottom); **D:** In situ contractile force measurements from preload-force tests on control limbs (left) and IR limbs (right) at day 6 (top) and day 12(bottom); **E:** In situ contractile force chart showing contractile force and duration of contraction between day 6 and day 2 tests.

4.2 Injured muscle from UCHL1 smKO has better morphology

To examine how UCHL1 affects muscle injury, we subjected flox control and UCHL1 smKO mice to hindlimb IR injury and measured muscle morphology using H&E staining in tibialis anterior (TA) muscle sections. H&E staining showed that IR-injured muscle from UCHL1 smKO mice had visibly less damaged muscle fiber bundles and less leukocyte infiltration when compared to the injured muscle of control mice (Fig 10). Given the absence of centrally-located nuclei within the muscle fibers of IR sections from UCHL1 smKO mice, the data suggests that muscle of UCHL1 smKO mice may be more resistant to damage than control mice.

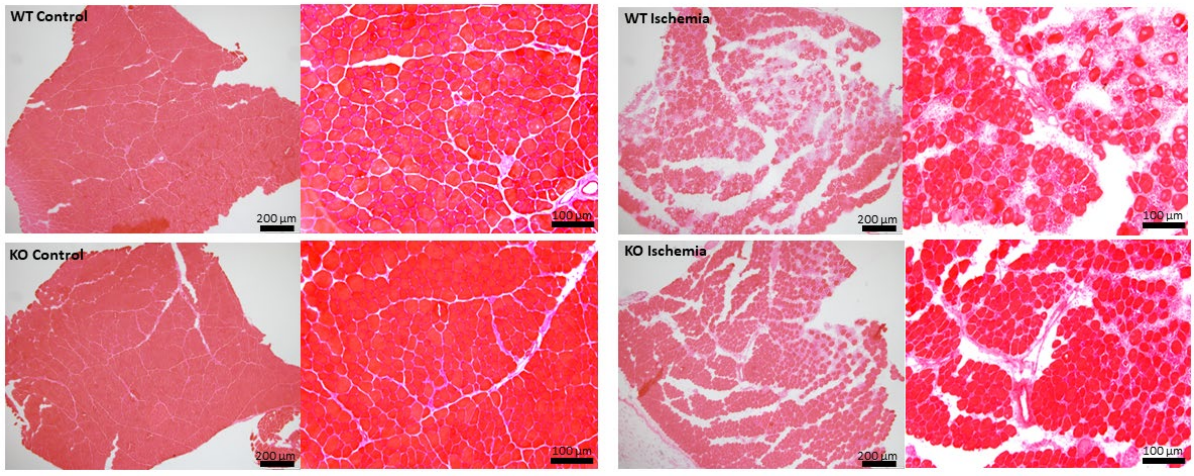

Figure 10: The effects of UCHL1 smKO following IR injury. **A:** H&E staining images of TA muscle sections taken from control mice (top) and UCHL1 smKO mice (bottom). Both control (left) and IR (right) limbs are represented at 4x (left side) and 10x (right side) magnifications 7 days after injury.

4.3 UCHL1 smKO mice have upregulated myogenic factors following injury

To further examine the effects of UCHL1 on regeneration of injured muscle, western blot and qPCR were used to look at myogenic markers. Myogenin protein level in IR muscle was no different between control and UCHL1 smKO mice at day 3, but was significantly upregulated in UCHL1 smKO mice at day 7 after injury.

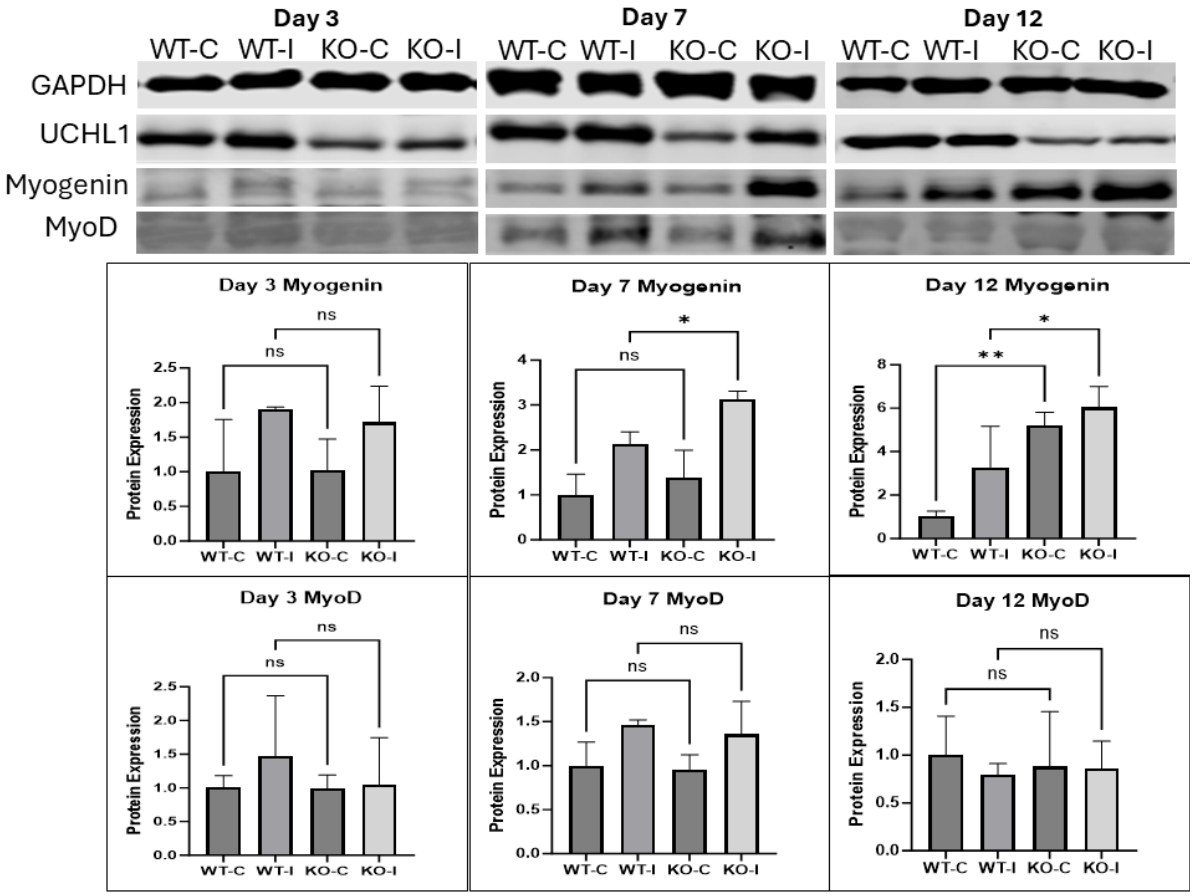

Figure 11: Myogenin protein is upregulated in UCHL1 smKO mice after injury. Raw images and quantification of western blots for GAPDH, UCHL1, myogenin, and MyoD from WT control, WT ischemia, UCHL1 smKO control, and UCHL1 smKO ischemia samples at days 3 (left), 7 (middle), and 12 (right) after injury; *P<0.05, n=3 mice per time point per genotype.

Interestingly, the knockout mice exhibited significantly increased Myogenin protein expression in both the control and injured muscle at day 12 when compared to control mice (Fig 11), suggesting that without UCHL1 inhibition, the injury signal can trigger myogenic activity in the injured site as well as remotely.

QPCR showed that myogenin mRNA expression was significantly upregulated in injured muscle of UCHL1 smKO mice compared to control mice both at day 3 and day 7 (Fig 12). These results confirm that UCHL1 smKO leads to an increase in myogenic activity after IR injury. The protein level of MyoD, an early stage myogenic marker of proliferation, was no different between control and UCHL1 smKO mice at 3 days and 7 days after injury, suggesting that UCHL1 may regulate differentiation in adult skeletal muscle regeneration differently from that in myoblasts. Together, the data suggests that myogenic signaling is activated at an earlier time point in UCHL1 smKO mice, and remains significantly more active during

reperfusion.

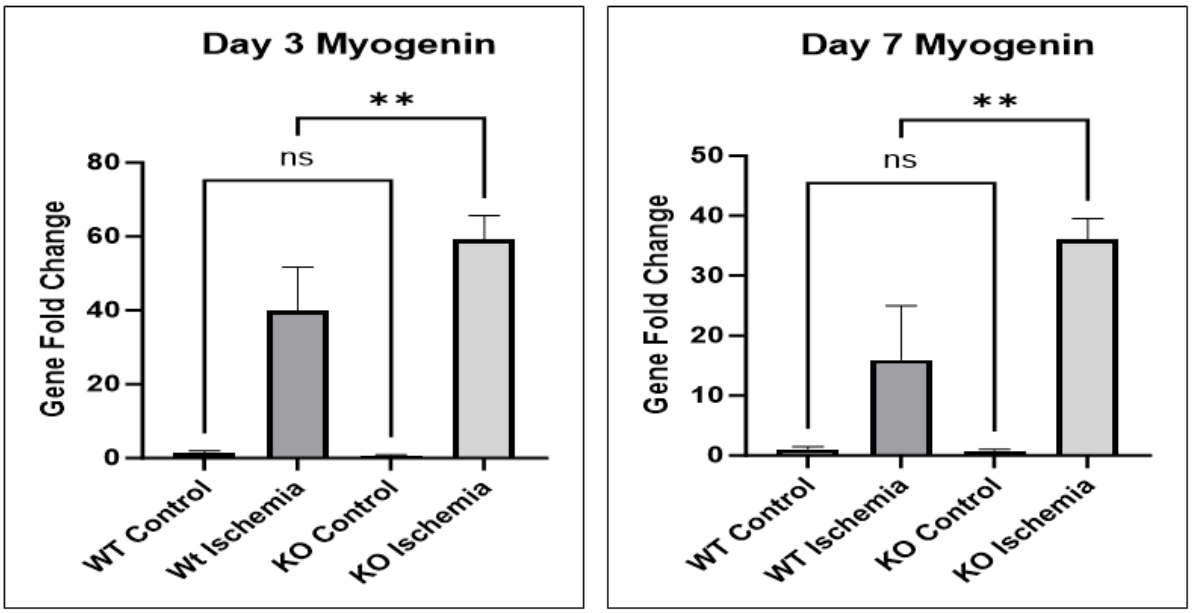

Figure 12: Myogenin RNA is upregulated in UCHL1 smKO mice following injury. Quantification of qPCR for myogenin cDNA in WT control, WT ischemia, UCHL1 smKO control, and UCHL1 smKO ischemia plantaris samples from days 3 and 7; *P<0.05, n=3 mice per group per genotype.

4.4 UCHL1 smKO improved functional recovery of injured muscle

To test whether UCHL1 also has an effect on muscle function recovery following skeletal muscle injury, control and UCHL1 smKO mice were subjected to *In situ* contractile force testing 12 days after IR injury. The injured gastrocnemius-plantaris complex in the UCHL1 smKO mice had significantly increased contractile force (Fig 13.A and 13.B) across several different contractile tests including preload-force (Fig 13.C), frequency-force (Fig 13.D), and amplitude force tests (Fig 13.E) when compared to the injured muscle complex in control mice, suggesting that UCHL1 smKO improves muscle functional recovery after IR injury.

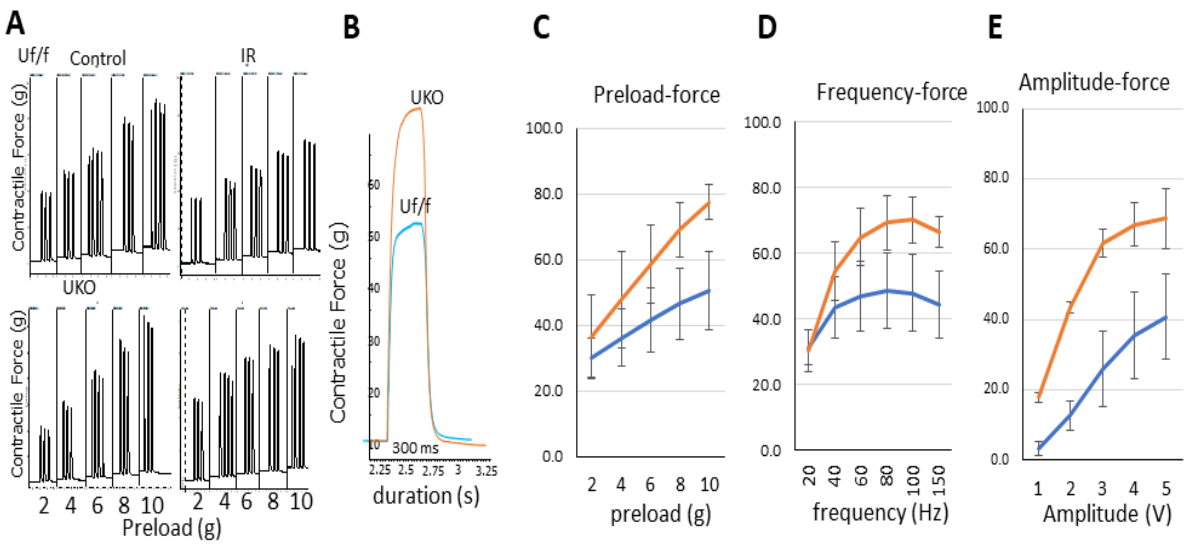

Figure 13: UCHL1 smKO improves function recovery following IR injury. **A:** Raw charts of preload-force contractile tests comparing control (left) and IR (right) limbs from WT (top) and smKO mice (bottom); **B:** Graph of mean contractile force over contraction duration comparing IR limb performance between WT and smKO mice; **C:** Chart of mean contraction from preload-force test comparing IR limb from smKO (orange) and WT (blue) mice; **D:** Chart of mean contraction from frequency-force test comparing IR limb from smKO (orange) and WT (blue mice; **E:** Chart of mean contraction from amplitude-force test comparing IR limb from smKO (orange) and WT (blue) mice.

4.5 UCHL1 negatively affects Pink1 activity

One of the major mechanisms by which IR injury can cause tissue damage is oxidative stress. To induce oxidative stress *in vitro*, similar to the effects of IR injury *in vivo*, differentiating control and UCHL1 knockdown myotubes were treated with hydrogen peroxide. Western blot showed that UCHL1 became upregulated during oxidative stress, similar to the results seen during IR injury *in vivo* (Fig 14). Additionally, despite myogenin being decreased upon hydrogen peroxide treatment, UCHL1 KD cells exhibited increased myogenin during oxidative stress when compared to control cells. Furthermore, treated UCHL1 KD cells had significantly increased phosphorylated Pink1, a major regulator of mitophagy, when compared to treated control cells. However, parkin, a downstream protein of Pink1, was not significantly different between treated control and knockdown cells. DRP1, the regulator of mitochondrial fission, was also not significantly different between treated control and KD cells. Lastly,

superoxide dismutase-2 (SOD2), a mitochondrial matrix protein responsible for suppressing ROS, was also not significantly different between the control and UCHL1 knockdown cells.

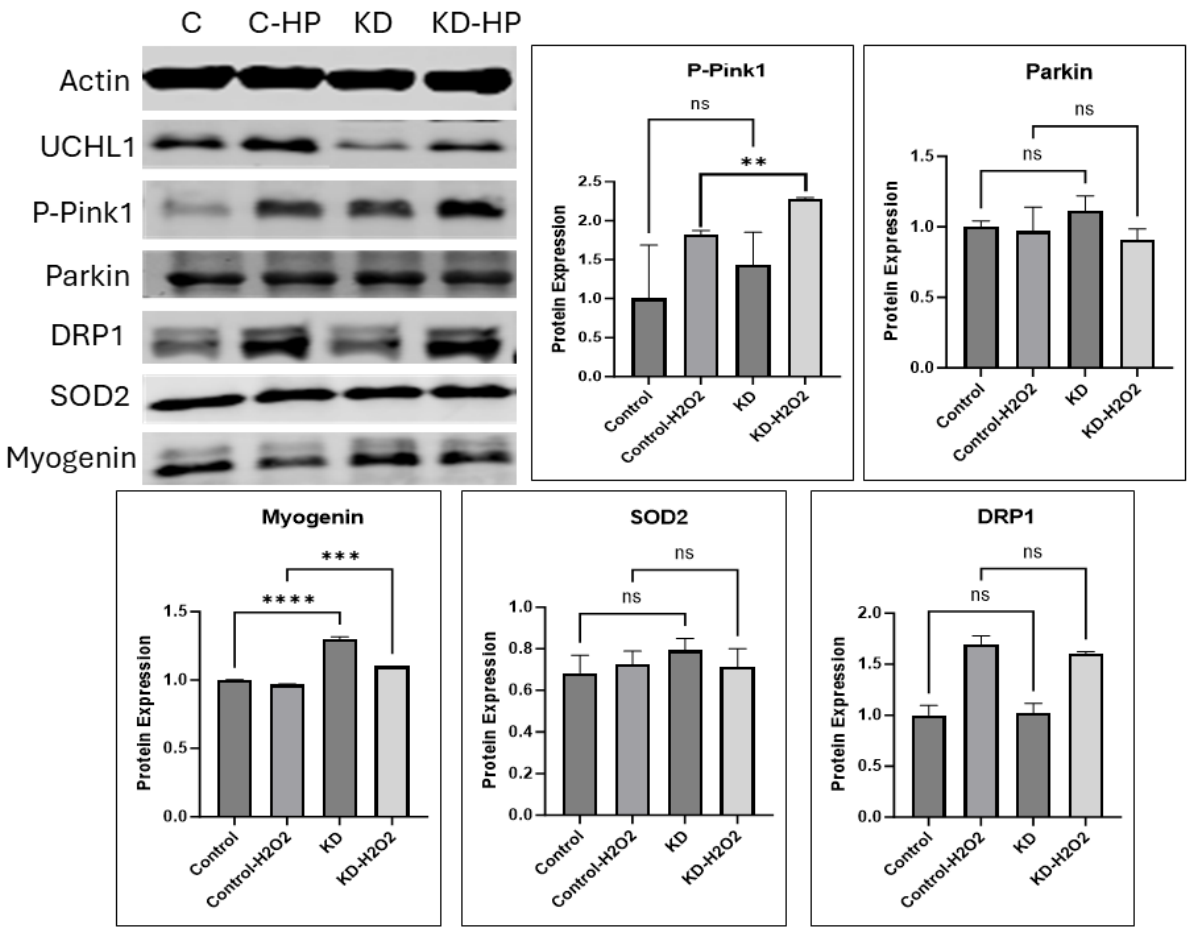

Figure 14: Pink1 phosphorylation is upregulated in UCHL1 KD myotubes during oxidative stress. Raw images and quantification from western blots for beta-actin, UCHL1, phosphor-Pink1, parkin, DRP1, SOD2, and myogenin between control and UCHL1 KD cells with or without hydrogen peroxide (HP, H2O2) treatment; *P<0.05, n=2 dishes per group.

Given the upregulation of Pink1 phosphorylation in UCHL1 knockdown myotubes during oxidative stress *in vitro*, we assessed whether UCHL1 affects Pink1 and other mitophagic markers during ischemia reperfusion injury *in vivo* using UCHL1 smKO and control mice. Western blot showed that none of the previous mitophagy markers were changed at day 3 between control and UCHL1 smKO mice. (Fig 15.A); however, phospho-Pink1 and parkin were both significantly increased in injured muscle of UCHL1 smKO mice at day 7 when compared to control mice, but DRP1 was unchanged (Fig 15 A). At day 12, parkin

remained significantly increased in injured muscle of UCHL1 smKO mice, and DRP1 was now also significantly increased in both control and injured muscle of UCHL1 smKO mice when compared to control mice (Fig 15.B). Together, the *in vitro* and *in vivo* data suggest that UCHL1 negatively regulates

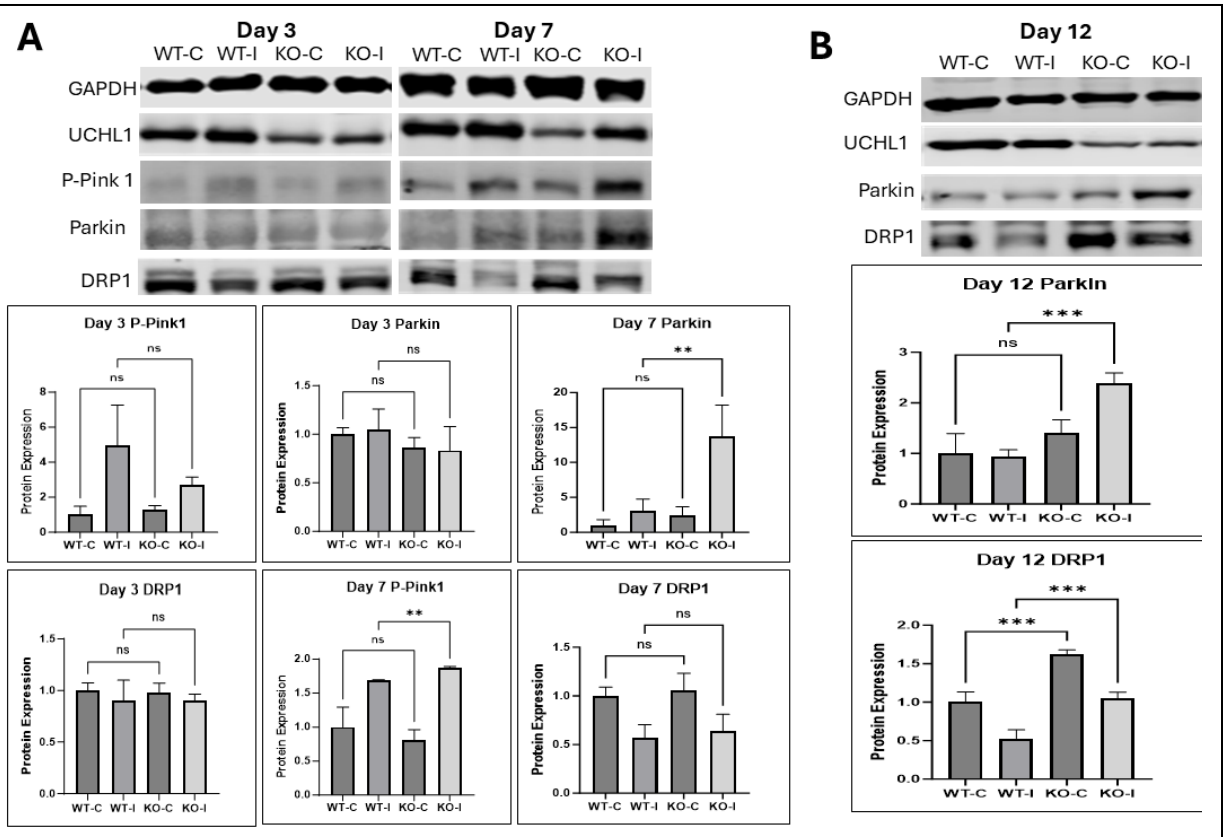

Figure 15: IR injury causes increased expression of mitophagy markers in UCHL1 smKO mice. **A:** Raw images and quantification from western blots for GAPDH, UCHL1, phosphor-Pink1, parkin, and DRP1, between WT control, WT ischemia. UCHL1 smKO control, and UCHL1 smKO ischemia samples at days 3 and 7 after injury; **B:** Raw images and quantification from western blots for GAPDH, UCHL1, parkin, and DRP1, between WT control, WT ischemia. UCHL1 smKO control, and UCHL1 smKO ischemia samples at day 12 after injury; *P<0.05, n=3 mice per group per time point.

Pink1 signaling activity during IR injury and recovery. Pink1 plays a critical role in mitophagy. Differentiation of myogenic precursors into mature myofibers increases energetic demand and requires significant remodeling of the mitochondrial network[79]. Mitophagy, the special autophagy involved in mitochondrial quality control, is crucial for mitochondrial clearance and biogenesis, and is essential for mediating pathophysiological processes following ischemia-reperfusion injury[79,83]. The effect of UCHL1 on Pink1 activity shown in the above in vitro and in vivo studies suggests a possibility that the promotion of

myogenesis and regeneration by UCHL1 KD/smKO may involve mitophagy; however, this requires further investigation.

4.6 UCHL1 affects mTOR-AKT signaling activity

It has been shown that phosphorylation of AKT at S473 regulates Pink1 activity[92]. To examine how UCHL1 regulates myogenesis, potentially through upregulated mitophagy, we looked at signaling proteins of the AKT signaling pathway. Western blot showed that at 3 days after IR injury, phosphorylated AKT (S473) was unchanged between control and UCHL1 smKO mice, but phosphorylated 4EBP1, a downstream signaling protein of mTORC1, was decreased in UCHL1 smKO mice (Fig 16). At day 7, phosphorylated AKT becomes upregulated in UCHL1 smKO mice, whereas phosphorylated 4EBP1 was not significantly changed when compared to control mice. At day 12, phosphorylated AKT remained upregulated in UCHL1 smKO mice when compared to control mice. Interestingly, phosphorylated 4EBP1 was also upregulated in UCHL1 smKO mice when compared to control mice. It is known that mTORC1 phosphorylates 4EBP1 whereas mTORC2 phosphorylates AKT at S473. This data suggests that during IR injury and regeneration, skeletal muscle UCHL1 regulates mTORC1 and mTORC2 activities in a time-dependent manner. At the early stages of injury (3 days after), UCHL1 smKO reduces mTORC1 activity, indicated by reduced 4EBP1 phosphorylation, which may promote autophagy/mitophagy to remove damaged cells and mitochondria. During the regenerative phase (around 7 days after injury and beyond), UCHL1 smKO enhances mTORC2 activity, indicated by increased AKT phosphorylation at S473, which may promote functional recovery and regenerated skeletal muscle[152].

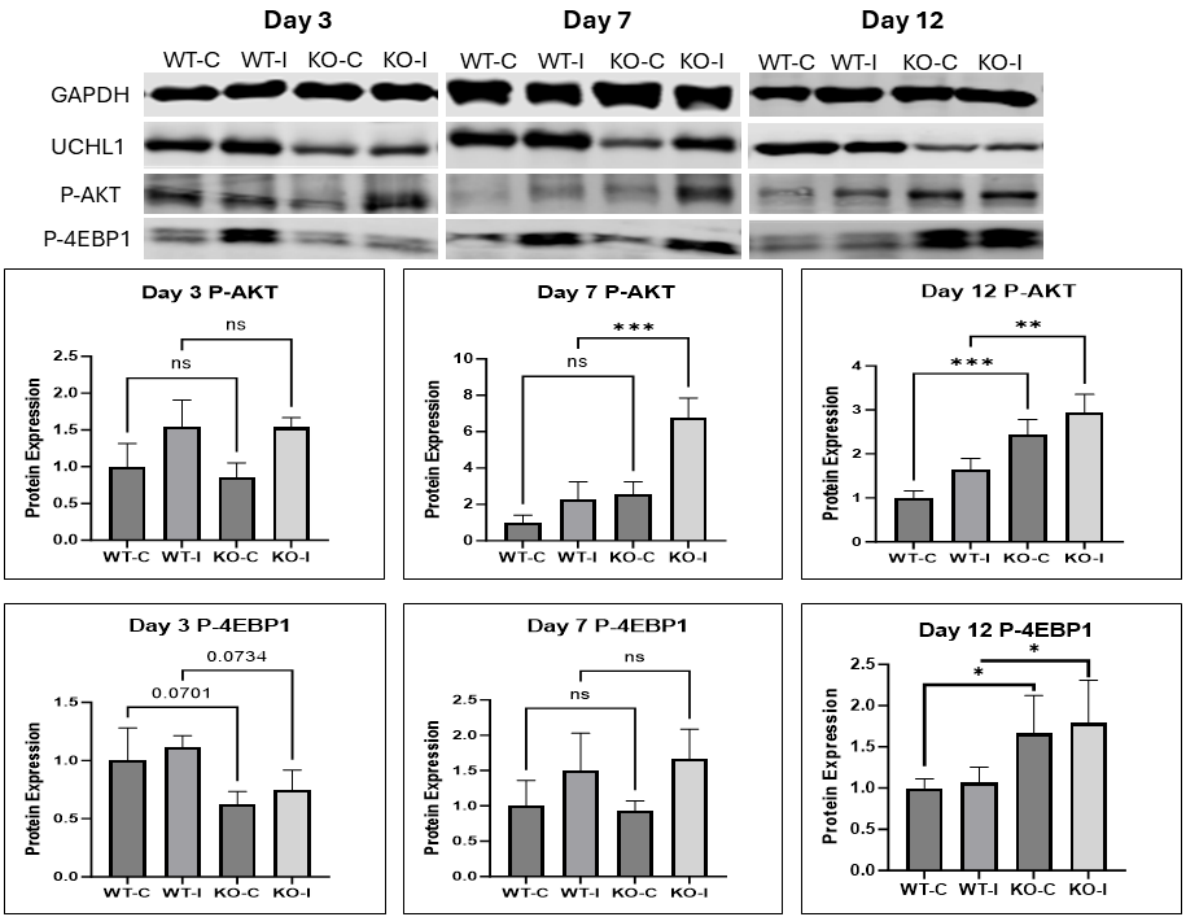

Figure 16: AKT signaling pathway activity is upregulated by UCHL1 smKO after injury. Raw images (top) and quantifications from western blots for GAPDH, UCHL1, phosphor-AKT (S473)(middle) and phosphor-4EBP1 (bottom) comparing WT control, WT ischemia, UCHL1 smKO control, and UCHL1 smKO ischemia samples at day 3, 7, and 12 after injury; *P<0.05, n=3 per group per time point.

4.7 The inflammatory response is altered in UCHL1 smKO mice

The inflammatory response, primarily driven by the innate immune response of the immune system, is essential for the maintenance of tissue homeostasis, ensuring tissue survival during infection, and healing following tissue injury[51]; however, inflammation can act as a double-edged sword by collaterally damaging healthy cells that would have otherwise been beneficial to the repair process[51,54,55]. Staining for CD11b revealed that UCHL1 smKO mice exhibited decreased infiltration of leukocytes 3 days after ischemic injury when compared to control mice (Fig 17.A). Specifically, staining for CD68 showed that UCHL1 smKO mice exhibited decreased infiltration of proinflammatory macrophages 3 days after ischemic injury when compared to control mice (Fig 17.B).

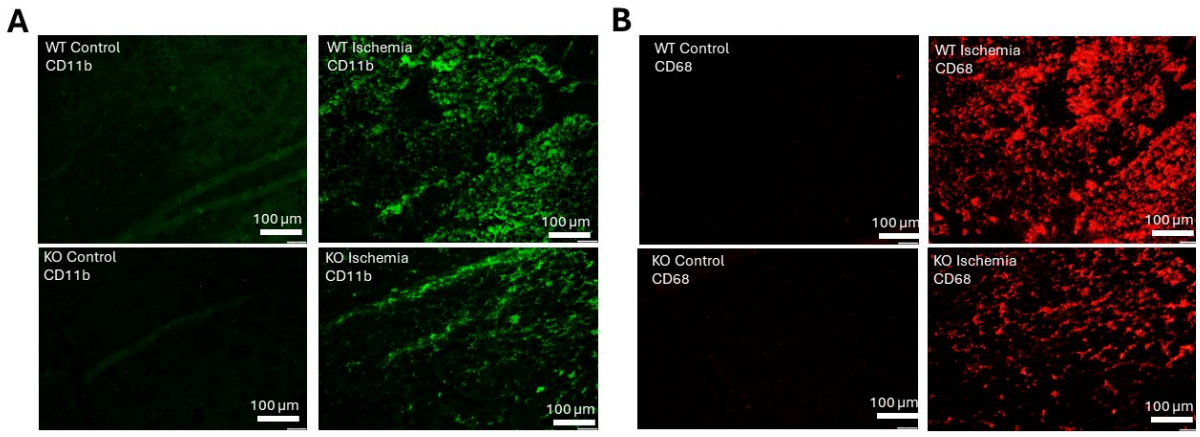

Figure 17: Macrophage and monocyte infiltration is decreased in UCHL1 smKO mice. Images of immunofluorescent staining for CD68 (A) and CD11b (B) between TA sections from control (left) and ischemic (right) hindlimbs of WT (top) and UCHL1 smKO (bottom) mice.

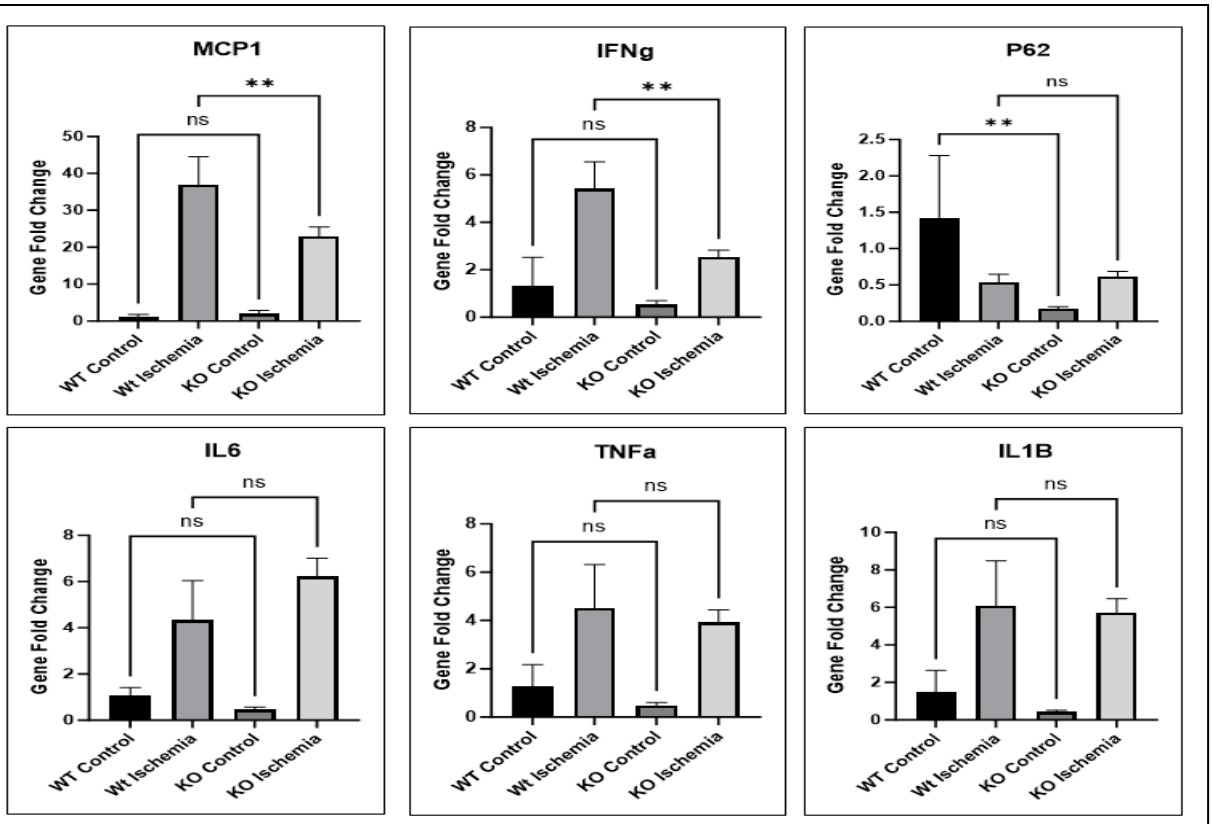

Figure 18: UCHL1 smKO mice exhibit decreased immune response biomarkers after injury. Quantification of qPCR for MCP1 (top left), IFNγ (top middle), P62 (top right), IL6 (bottom left), TNFα (bottom middle), and IL1β (bottom right) cDNA in WT control, WT ischemia, UCHL1 smKO control, and UCHL1 smKO ischemia plantaris samples from days 3 and 7; *P<0.05, n=3 mice per group per genotype.

Additionally, qPCR displayed significantly downregulated mRNA levels of monocyte chemoattractant protein-1 (MCP1) and Interferon gamma (IFNγ), key cytokines in the pro-inflammatory response, in damaged muscle from UCHL1 smKO mice after 3 days of reperfusion when compared to control mice; however, mRNA levels of IL1β, TNFα, and IL6 were not significantly different between genotypes (Fig 18). Interestingly, mRNA of P62, a critical receptor of autophagy and a positive regulator of inflammatory transcription factor NF-κB[82], was significantly decreased in control muscle of UCHL1 smKO mice, but not in ischemic muscle when compared to control mice. This data suggests that UCHL1 may be a positive regulator of the immune response. Additionally, the data indicates UHCL1 may regulate p62, which negatively impacts myogenesis

CHAPTER 5

Specific Aim #3 results

5.1 Manipulation of UCHL1 alters p62 expression

Following the previous results, we further investigated how p62 may be involved with UCHL1 and its regulation of myogenesis during development and regeneration. To examine this, UCHL1 was manipulated in C2C12 cells *in vitro* via UCHL1 knockdown, wildtype UCHL1 overexpression, and C90S mutant UCHL1 overexpression. Western blot showed that p62 was significantly decreased when UCHL1 was knocked down, and significantly increased when WT UCHL1 was overexpressed (Fig 19). Interestingly, p62 was not significantly different between control and the DUB activity deficient C90S UCHL1 overexpressed cells, suggesting that UCHL1 regulates p62 expression in C2C12 cells via deubiquitinating function.

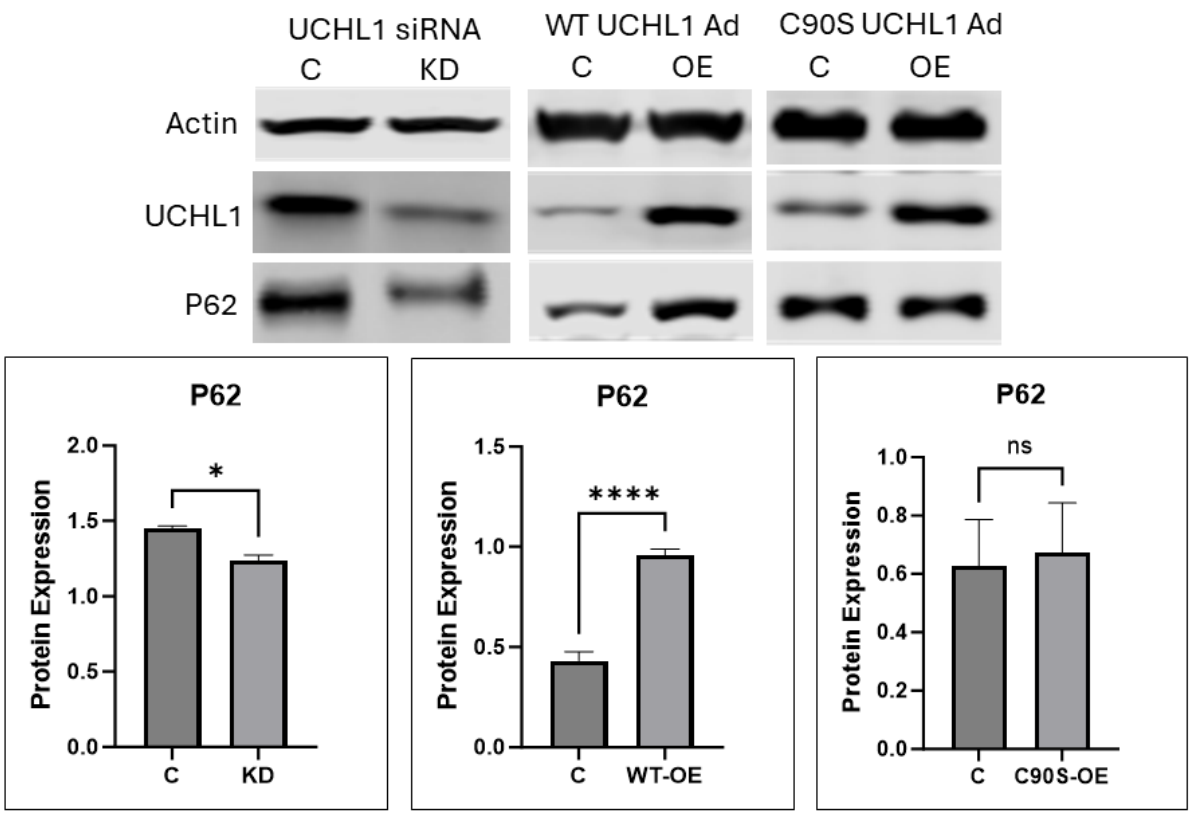

Figure 19: UCHL1 regulates P62 via DUB function. Raw images and quantification from western blots for beta-actin, UCHL1, and P62 comparing control cells with UCHL1 knockdown cells (left), wildtype UCHL1 overexpressed cells (middle), and C90S mutant UCHL1 overexpressed cells (right); *P<0.05, n=4 dishes per group.

To further assess the association between UCHL1 and p62, UCHL1 was overexpressed in C2C12 myoblasts with WT UCHL1 adenovirus expressing HA tag and upon collecting cells, p62 was immunoprecipitated. Using western blot, the presence of UCHL1 in the p62 IP sample highlighted the direct interaction between the two proteins (Fig 20). This data further supports that UCHL1 regulates p62 expression through direct DUB function.

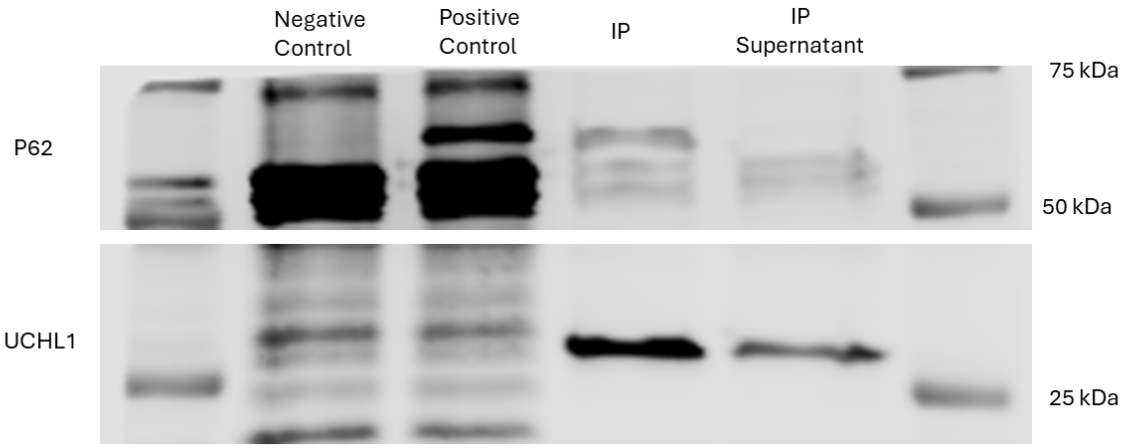

Figure 20: UCHL1 and P62 directly interact. Raw western blot images from Co-immunoprecipitation (IP) of P62 (top) and UCHL1 (bottom) in HA-UCHL1 overexpressed C2C12 myoblasts.

5.2 UCHL1 regulates p62 release

Studies have provided evidence that p62 is able to be secreted from cells as part of autophagy-related vesicle trafficking[89-91]. Given the relationship between UCHL1 and p62, we assessed whether UCHL1 knockdown results in downregulated p62 via degradation, or via release into the extracellular space. Data from a p62 ELISA assay showed that p62 is significantly higher in cell media from UCHL1 knockdown cells when compared to control cells (Fig 21.A). Consistent with this, serum from UCHL1 smKO mice also exhibited significantly increased levels of p62 when compared to serum taken from control mice (Fig 21.B). This data suggests that UCHL1 controls p62 release from muscle cells into the extracellular space.

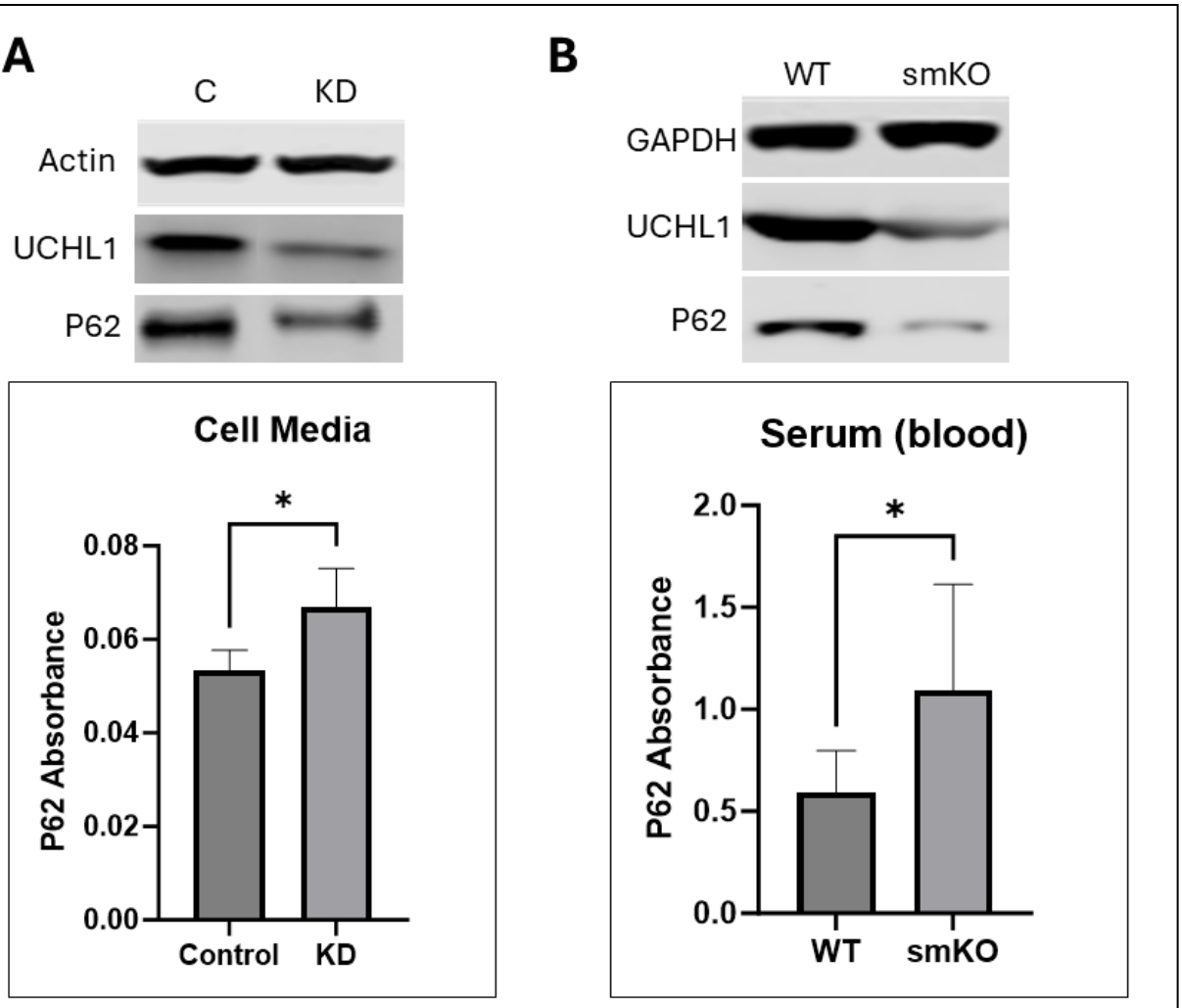

Figure 21: UCHL1 regulates extracellular P62 release. **A:** Raw western blot images (top) of beta-actin, UCHL1, and P62 between control and UCHL1 knockdown cells, and quantification of P62 enzyme-linked immunosorbant assay (ELISA) comparing control and UCHL1 knockdown cell media; **B:** Raw western blot images (top) of GAPDH, UCHL1, and P62 between WT and UCHL1 smKO mice, and quantification of P62 enzyme-linked immunosorbant assay (ELISA) comparing WT and UCHL1 smKO serum; *P<0.05, n=4 dishes, n=8 mice.

5.3 Myogenic factors are unaffected by extracellular p62

Given the fact that knockdown/knockout of UCHL1 in skeletal muscle cells and tissue results in upregulated myogenesis, as well as increased p62 secretion, we asked whether the released extracellular p62 may contribute to myogenesis. Under this notion, we examined how extracellular p62 affects myogenic factors by treating C2C12 cells with various concentrations of recombinant p62 protein. Western blot showed that myogenic factors myogenin and MyoD were not significantly changed by the

presence of extracellular p62 (Fig 22). Interestingly, extracellular p62 treatment significantly increased UCHL1 while intracellular p62 was significantly decreased. Signaling proteins of the mTOR pathway, which is associated with both UCHL1 and p62, were also blotted for. AKT and phosphor-4EBP1 were both significantly upregulated when cells were treated with recombinant p62. Surprisingly, DRP1, the regulator of mitochondrial fission, was also significantly upregulated in the presence of extracellular p62. The data gathered from this experiment suggests that extracellular p62 is unlikely to stimulate myogenesis, and thus the increased extracellular p62 by UCHL1 smKO likely does not contribute to the enhanced myogenesis. The data also further supports that UCHL1, p62, and the mTOR-AKT signaling pathway interact with one another.

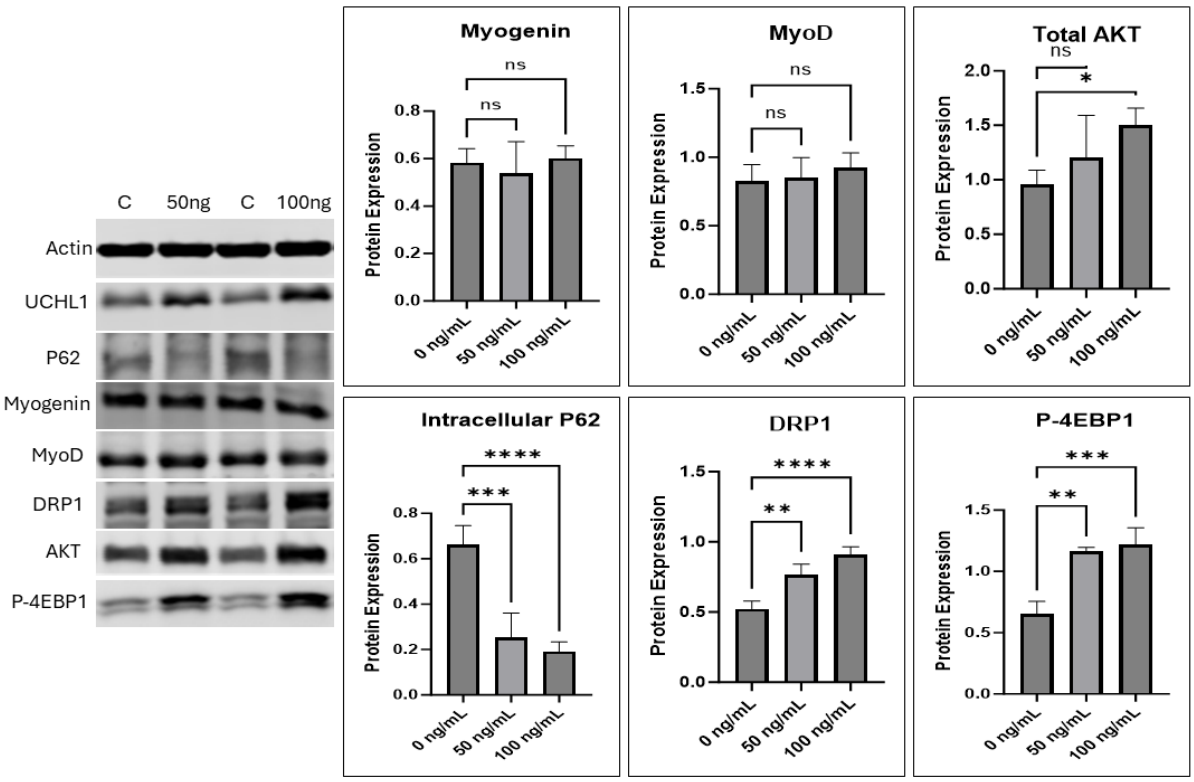

Figure 22: Extracellular P62 does not affect myogenic factor expression in vitro. Raw images (left) and quantifications from western blots for beta-actin, UCHL1, P62 (bottom left), myogenin (top left), MyoD (top middle), DRP1 (bottom middle), AKT (top right), and phosphor-4EBP1 (bottom right); *P<0.05, n=6, n=3, n=3.

CHAPTER 6

Summary and Discussion

UCHL1 was originally discovered as a brain-specific protein and its role in neuronal function has been well documented[1,93]; however, despite also being found in other tissue[7-9], the role of UCHL1 in skeletal muscle is still relatively unknown. The results from this study further supported that UCHL1 is a negative regulator of myogenesis, both during development and during regeneration after injury. The knockdown of UCHL1 increases myotube differentiation and upregulates myogenic factors *in vitro*. Furthermore, the absence of UCHL1 in skeletal muscle results in increased muscle fiber size during earlier stages of muscle maturation, and changes in fiber type specificity. During ischemia-reperfusion injury, the presence of UCHL1 significantly reduced myogenic factors, functional regeneration, and signals that regulate mitochondrial remodeling. Additionally, we have discovered that UCHL1 directly regulates P62 expression and secretion from skeletal muscle. These findings are significant due to the involvement of UCHL1 during development and regeneration, and they suggest that UCHL1 may be a potential therapeutic target for skeletal muscle injury.

6.1 UCHL1 negatively regulates myogenesis during skeletal muscle development

6.1.1 Downregulation of UCHL1 results in increased myoblast differentiation

Previous findings from our lab have reported that UCHL1 is involved in the regulation of both skeletal muscle oxidative activity and mTORC1 signaling activity, as well as playing a role in myogenic functions[17-21]. Our data displayed that knockdown of UCHL1 in C2C12 myoblasts resulted in increased differentiation, seen by significantly greater myotube width, across multiple time points throughout myoblast to myotube differentiation. Consistent with the previous work, this data supports that UCHL1 is a negative regulator of myogenesis, at least in part by partially inhibiting myoblast differentiation.

6.1.2 UCHL1 serves as an inhibitor of MRFs

Myogenic regulatory factors (MRFs) are critical for the process of myogenesis, ultimately driving myogenic progenitors through phases of proliferation and differentiation until healthy, mature myofibers are formed[33,34]. Two of the key MRFs, MyoD and myogenin, contribute significantly to myoblast proliferation myotube differentiation respectively[31-37]. As the data revealed, both of these myogenic

regulatory factors were significantly upregulated by UCHL1 knockdown across multiple timepoints in differentiating myotubes. Surprisingly, overexpression of UCHL1 also upregulated myogenin; this mechanism is unclear. It is possible that the overexpressed UCHL1 lacks DUB activity, causing a dominant negative effect similar to UCHL1 knockdown. Indeed, other studies have documented the involvement of UCHL1 in feedback loops with β-catenin[94], and other proteins[95-97], suggesting that it is possible for a UCHL1-myogenin regulatory feedback loop to be in place in skeletal muscle cells. These results further support that UCHL1 is a negative regulator of myogenesis, and potentially acts directly or indirectly through a negative feedback loop. Myosin, a motor protein of muscle, consists of subunits known as myosin heavy chain (MyHC) which provides energy needed for contraction, and myosin light chain (MyLC) which provides structural integrity[80,81]. Although the absence of UCHL1 upregulates myogenic factors and myotube differentiation in C2C12 contractile cells, the western blot data showed that UCHL1 had no significant impact on the expression of myosin heavy chain 1/2/4/6, embryonic myosin heavy chain, or neonatal myosin heavy chain. This in vitro data is inconsistent compared to the in vivo data from UCHL1 smKO mice. Studies have shown that myosin heavy chain can be regulated by thyroid hormone[98-100], suggesting the possibility that other cell types, such as follicular cells, may be needed in conjunction with C2C12 cells for any regulatory affect to be seen via UCHL1 manipulation.

6.1.3 Skeletal muscle knockout of UCHL1 results in accelerated muscle fiber growth and altered myosin heavy chain expression

Skeletal muscle is a diverse organ, making up 40% of body mass and is responsible for many functions including locomotion, metabolism, thermogenesis, and energy homeostasis[22-24]. UCHL1 skeletal muscle specific knockout (smKO) mice were used to assess the impact of UCHL1 on muscle fiber development *in vivo*. Our data showed that muscle fiber size was significantly larger in UCHL1 smKO mice at 1 and 2 months of age compared to control mice, but fiber size was not significantly different between the two strains at 3 months of age. Judging by the amount of respective growth month to month, we see that between 2 and 3 months of age, the UCHL1 smKO mouse muscle fibers do not grow much whereas the control mice exhibit a much larger increase in muscle fiber size month to month. This data suggests that the muscle fiber size of UCHL1 smKO mice begins to plateau at 2 months, allowing the fiber size of control mice to catch up to that of UCHL1 smKO mice by 3 months of age. These results

support the notion that during normal development, UCHL1 is a negative regulator in skeletal muscle fiber differentiation and maturation, but may not be crucial for adult muscle mass maintenance.

Muscle fibers themselves are divided into several types based on contractile properties and physiological features[25,28]. Type 1 muscle fibers are referred to as slow twitch fibers, being slow to contract and fatigue, and relying on oxidative metabolism for energy requirements. Type 2 fibers are commonly referred to as fast twitch fibers with type 2b fibers exhibiting fast contraction, quick fatigue, and relying on glycolytic metabolism, and type 2a fibers being an intermediate between types 1 and 2b, relying on a mix of oxidative and glycolytic metabolism, and having fast contraction with slower fatigue[25-28]. Fiber type staining of the tibialis anterior (TA), a muscle composed of mainly type 2 fibers[101], showed a large increase of type 2b fibers in UCHL1 smKO mice when compared to control mice. Staining also revealed a slight decrease in type 2a fibers in the UCHL1 smKO mice. It has been shown that UCHL1 is primarily expressed in oxidative muscle fibers[19]. With this in mind, it is likely that the skeletal muscle knockout of UCHL1 results in decreased type 1 and type 2a fibers due to their oxidative functions, and a fiber type switch to type 2b as a compensatory mechanism. Western blot for myosin heavy chain and fiber type expression made things even more interesting. We observed that UCHL1 smKO mice had increased MyHC in the soleus, a predominantly type 1 muscle, at 1 and 2 months, and significantly decreased MyHC in the EDL, a predominantly type 2b muscle, at 1 and 2 months; however, MyHC at 3 months was indifferent between UCHL1 smKO mice and control mice in both the soleus and EDL. Western blot for type 1 fibers showed no difference between control and UCHL1 smKO mice at 1 and 2 months in the soleus, but a significant increase in type 1 fiber expression at 3 months. Oppositely, type 1 fiber expression was decreased in the EDL of UCHL1 smKO mice across all time points. The results from this study suggest that UCHL1 may not only be expressed in oxidative fibers as we had originally thought, and that UCHL1 plays diverse roles in the regulation of fiber types during developeent.

Overall, the results of this aim support that UCHL1 is indeed a negative regulator of myogenesis during skeletal muscle development via upregulation of myogenic factors. Furthermore, the data collected highlights the role of UCHL1 as it pertains to fiber type specificity, and suggests that UCHL1 is involved in skeletal muscle metabolism, potentially contributing to the upregulation of muscle growth.

6.2 UCHL1 is a negative factor in muscle regeneration

Aside from development of muscle tissue, myogenesis serves a critical role through the regeneration of injured muscle and turnover of muscle cells. Similar to embryonic muscle development, regeneration of adult muscle relies on the proliferation and differentiation of myogenic precursors; however, unlike embryonic development, adult muscle myogenesis is driven by the activation of already present quiescent stem cells which migrate to the site of injury at the basal lamina, or to adjacent myofibers if the basal lamina is destroyed[33,35]. Skeletal muscle injuries are common and can be sustained from various causes including direct trauma, neurological diseases, and ischemia caused by surgeries that utilize tourniquet application[38]; in fact, ischemia-reperfusion injury is the most common type of skeletal muscle injury[39,40,43,44].

6.2.1 Regeneration is significantly increased in UCHL1 smKO mice

To obtain a better understanding of how UCHL1 affects regeneration following injury, we again looked at myogenic regulatory factors MyoD and myogenin in UCHL1 smKO mice after IR. Interestingly, UCHL1 becomes upregulated in injured muscle throughout the regenerative process, as do the myogenic regulatory factors, providing further evidence of the link between UCHL1 and myogenesis. We observed no significant difference in myogenin or MyoD expression between control and UCHL1 smKO mice at day 3, though this was somewhat expected as a significant amount of inflammation is present during this time point. At day 7 of reperfusion, injured tissue from UCHL1 smKO mice exhibited significantly increased expression of myogenin when compared to injured muscle from control mice, but no difference in MyoD expression was seen between the two strains. 12 days after injury, UCHL1 smKO mice showed increased expression of myogenin in both control and injured muscle when compared to control mice; however, MyoD expression was still unchanged between the two groups. Based on the increased expression of myogenin in UCHL1 smKO mice after injury, myogenin RNA was also analyzed using qPCR. Unlike western blot from day 3, qPCR on day 3 showed that myogenin was significantly greater in injured muscle of UCHL1 smKO mice, and continued to be upregulated through day 7 compared to control mice. This data suggests that UCHL1 partially inhibits myogenesis following skeletal muscle injury, at least via the negative regulation of myogenin, and that myogenic signaling activity begins earlier in UCHL1 smKO mice.

To further assess the affects of UCHL1 on muscle regeneration following injury, mice were subjected to contractile force testing 12 days after IR injury. Using the preliminary data obtained from the development of our IR injury model, day 12 of reperfusion was chosen as the muscle was almost completely healed and could withstand prolonged contractile tests. Using several different stimuli tests including various preload, frequency, and voltage, the results showed that injured muscle from UCHL1 smKO mice had significantly better contractile function when compared to injured muscle from control mice. This data also supports that UCHL1 smKO mice have increased regenerative capabilities following skeletal muscle injury.

6.2.2 UCHL1 smKO muscle retains better morphology after injury

In day 7 post-injury muscle stained with H&E, further analysis showed a lack of centrally located nuclei in muscle fibers of the UCHL1 smKO injured fibers. Centrally located nuclei are a sign of newly regenerated fibers[102-105]. Knowing this, the data suggests that UCHL1 smKO mice may be more resistant to damage caused by IR injury. Additionally, given the reliance on oxidative and glycolytic metabolism in different fiber types, the data may suggest that predominantly type 2b muscles, such as the TA and EDL, are more resistant to hypoxic damage during periods of ischemia where anaerobic metabolism can be utilized[106], and even more so considering the more significant concentration of type 2b fibers within these muscles observed in UCHL1 smKO mice. Therefore, the better outcome after IR injury seen in UCHL1 smKO mice may not only be due to the enhanced regeneration, but also due to more resistance to injury. Further studies are needed to support these claims.

Overall these results further suggest that UCHL1 is not only a negative regulator in normal muscle development and growth, but also elicits inhibitory effects in post injury regeneration, and therefore, can be a potential therapeutic target for muscle injury and regeneration.

6.2.3 UCHL1, mTOR, and mitophagy related signaling

Damaged and depolarized mitochondria are selectively eliminated via the autophagy-lysosome system, a process known as mitophagy. Mitophagy is a critical process for skeletal muscle myogenesis and regeneration[107,108], and enhanced mitophagy has been found to improve both mitochondrial health and skeletal muscle function[109]. Using hydrogen peroxide to induce oxidative stress *in vitro*, our data showed that UCHL1 was again upregulated in treated cells, similar to what can be seen during IR injury *in*

vivo. Western blot also showed that phosphorylation of Pink1, a key regulator of mitophagy, was significantly increased in treated UCHL1 KD cells; however, parkin, a downstream protein of Pink1 and another key regulator of mitophagy, was no different between treated control and KD cells. Additionally, mitochondrial dynamin-related protein-1 (DRP1), the regulator of mitochondrial fission, was also no different between control and UCHL1 knockdown cells. Western blot also showed that superoxide dismutase 2 (SOD2), a mitochondrial suppressor of reactive oxygen species, was unchanged between control and knockdown cells. This in vitro data suggests that UCHL1 is a negative regulator of Pink1, a key mitophagy factor. However, since other mitophagy markers were unchanged by UCHL1 KD, the role of UCHL1 in mitophagy in our in vitro model is unclear.

Mitophagy markers were also looked at during regeneration following IR injury. Western blot showed that none of the markers were significantly different between control and smKO mice at day 3. At day 7, both phosphorylated Pink1 and parkin had significantly increased expression in injured muscle of UCHL1 smKO mice when compared to control mice, although DRP1 was not significantly different. 12 days after injury, parkin remained upregulated in injured muscle from UCHL1 smKO, and DRP1 became significantly increased in both control and injured limbs of smKO mice when compared to control mice. These results suggest that UCHL1 also negatively regulates mitophagy, and that upregulated mitophagy observed in UCHL1 smKO mice may contribute to increased regenerative capabilities.

Pink1 activity is regulated by phosphorylation of AKT at S473[92]. We wanted to determine a mechanism for UCHL1's regulation of mitophagy which likely contributes to the upregulation of myogenesis seen in UCHL1 smKO mice. Western blot showed no significant difference in AKT S473 phosphorylation between control and smKO mice at day 3. At day 7, AKT phosphorylation was upregulated in injured muscle of UCHL1 smKO mice and remained upregulated at day 12 when compared to injured muscle from control mice. Interestingly, phosphorylation of 4EBP1, a downstream target of mTORC1, was decreased in injured muscle of smKO mice at day 3, no different at day 7, and significantly increased at day 12 when compared to injured muscle of control mice. These results offer novel information on the dynamic effects of UCHL1 in different stages of injury and recovery. During the early stages of injury recovery (3 days after), UCHL1 may be essential for mTORC1 activity. UCHL1

smKO reduces mTORC1 activity, indicated by reduced 4EBP1 phosphorylation, which may promote autophagy/mitophagy to remove damaged cells and mitochondria. During the regenerative stages of injury recovery (around 7 days and beyond), UCHL1 may be inhibitory for mTORC2 activity. UCHL1 smKO enhances mTORC2 activity, indicated by increased AKT phosphorylation at S473, which may promote functional recovery and regeneration of skeletal muscle[152].

Overall, these results suggest that UCHL1 has an inhibitory effect on injury recovery and muscle regeneration via regulation of mTOR and its downstream signals in a dynamic manner.

6.2.4 UCHL1 smKO elicits an altered inflammatory response following injury

Following the previous results, we examined if the immune response was indeed altered by UCHL1 during the regeneration process. Immunofluorescent staining with CD68 showed that pro-inflammatory macrophage infiltration was decreased in injured muscle of UCHL1 smKO mice at day 3 when compared to control mice. Additionally, staining with CD11b, a surface marker of natural killer cells, granulocytes, and macrophages[121], also showed decreased leukocyte infiltration in injured muscle of UCHL1 smKO mice at the same time point. This suggests that UCHL1 may positively regulate the immune response following injury. As previously stated, inflammation can be detrimental by collaterally killing healthy cells that would otherwise assist in regeneration, thus, the decreased immune response could potentially fast-track when myogenesis begins. In addition, the data also suggests that UCHL1 smKO muscle is indeed more resistant to damage (depending on the muscle complex) and the less damaged muscle triggers a lesser immune response compared to control mice. Further studies are needed to support or refute these claims.

Immune cell markers were also analyzed using qPCR to better understand how UCHL1 potentially affects the immune response. Cytokines involved with the migration and activation of macrophages/monocytes, those being MCP1 and IFNγ respectively, had significantly downregulated levels of cDNA in injured muscle from UCHL1 smKO mice when compared to that of control mice. Il-6 and IL-1β, other cytokines involved in the inflammatory response, were not significantly different between injured muscle of control and knockout mice. This data suggests that UCHL1 may be a positive regulator of the immune response via macrophage activity; this hypothesis is supported by recent studies

documenting the role of UCHL1 as a regulator of macrophage activity in regards to inflammation[122,123]. We also looked at P62 cDNA, a multifunctional scaffold protein associated with the mTOR signaling pathway which acts as a receptor of autophagy and mediator of inflammation[89-91, 124-128], and saw that P62 cDNA was significantly downregulated in UCHL1 smKO control muscle, but not injured muscle when compared to control mice. This suggests that P62 is regulated by UCHL1, and that UCHL1 may affect mitophagy and the immune response via P62, ultimately resulting in mediation of myogenesis.

The results of aim 2 support that in addition to muscle development, UCHL1 is also a negative regulator of skeletal muscle myogenesis during regeneration following injury such as ischemia-reperfusion. The results also suggest that UCHL1 is a negative regulator of mTOR signaling pathway activity which likely contributes to the upregulation of myogenesis seen in UCHL1 smKO mice. The data further suggests that UCHL1 positively mediates macrophage activity during inflammation, and that the UCHL1 may regulate p62, potentially leading to the aforementioned downstream effects.

6.3 UCHL1 regulates p62 expression and release

6.3.1 UCHL1 directly regulates p62 expression

To determine whether UCHL1 does indeed regulate p62 expression, UCHL1 was manipulated *in vitro* using siRNA knockdown and adenovirus overexpression in C2C12 cells. Western blot showed that p62 expression was decreased when UCHL1 was knocked down, and p62 expression was increased when wildtype UCHL1 was overexpressed. This data supports that UCHL1 regulates p62 expression. To further examine this regulatory mechanism, C90S mutant UCHL1, which has impaired deubiquitinase function[129], was also overexpressed in C2C12 cells. Interestingly, there was no significant change in p62 expression in C90S overexpressed cells. These results suggest that UCHL1 regulates p62 expression through deubiquitinase function. Recent studies have shown that other deubiquitinating enzymes, USP8,

USP13, and USP20, stabilize p62 via DUB function[130-132]. It is likely that the absence of UCHL1 in knockdown/knockout causes p62 to become ubiquitinated and degraded by the UPS[133], resulting in decreased expression. To further examine the association between UCHL1 and p62, C2C12 cells were overexpressed with WT UCHL1 adenovirus expressing HA tag and p62 was immunoprecipitated. Western blot results of this co-IP with UCHL1 highlighted the direct interaction between the two proteins, supporting that UCHL1 indeed directly regulates p62 expression by DUB function.

6.3.2 Extracellular p62 release is regulated by UCHL1

Following the previous results, we wanted to determine the fate of p62 as recent studies have provided evidence that p62 is able to be secreted from cells as part of autophagy-related vesicle trafficking[89-91]. It was revealed that cell media from UCHL1 KD cells contained significantly higher levels of p62 when compared to control cells. This was also examined *in vivo*, and serum collected from UCHL1 smKO mice also had significantly higher p62 content compared to control mice. This data suggests that UCHL1 regulates release of p62 into extracellular space. Given the previous results, we can hypothesize that ubiquitination of p62 by UCHL1 KD/smKO results in release from the cell rather than degradation via the UPS. p62 has been identified as a regulator of the metabolic shift during myoblast differentiation[134,135]. Moreover, extracellular p62 has also been identified as a mediator of inflammation and septic cell death[136,137]. This raises the question of whether extracellular p62 is contributing to the cellular responses seen during IR injury in UCHL1 smKO mice.

To answer this question, differentiating C2C12 cells were treated with recombinant p62 protein (rP62) to mimic the environment of extracellular p62 *in vivo*. Very similar to what we saw with hydrogen peroxide treatment and IR injury, UCHL1 protein expression was increased in the presence of extracellular p62, suggesting that similar signaling pathways are active during oxidative stress and in the presence of extracellular p62, as well as supporting that UCHL1 is a critical mediator of cellular functions in these conditions. Furthermore, intracellular p62 expression was significantly decreased in cells that were treated with rP62. There are several possibilities for this phenomenon. Considering that nature of UCHL1, one possibility is that the cells upregulate UCHL1 due to the external stimuli in order to regulate intracellular homeostasis by removing ubiquitin from downstream proteins of p62-dependent signaling pathways[138-140]. Another possibility revolves around the Wnt signaling pathway. Much like the mTOR-AKT

pathway, the Wnt signaling pathway is also involved in the activation of myogenic regulatory factors[141-144]. Studies have shown that β-catenin, a downstream protein of the Wnt pathway, forms a complex with UCHL1 in a positive regulation loop, being able to upregulate the expression of one another[145-147]. Moreover, overexpression of p62 results in activation of the Wnt signaling pathway[148,149], and β-catenin acts as a repressor of p62 expression[150,151]. With all that in mind, it is possible that the already active Wnt signaling pathway during regeneration/development becomes increasingly active given the abundance of extracellular p62 which in turns upregulates β-catenin and UCHL1 expression, effectively repressing intracellular p62 expression. More studies are needed to better understand this mechanism. Western blot also showed that neither MyoD or myogenin were significantly different between treated and untreated cells, suggesting that neither the absence of intracellular p62 nor the surplus of extracellular p62 as a result of UCHL1 smKO upregulate myogenesis directly. Surprisingly, DRP1 protein expression was significantly increased by extracellular p62. Given the increased expression of extracellular p62 and decreased expression of intracellular p62 similar to that of UCHL1 smKO mice after injury, this data supports that UCHL1 negatively regulates the release of p62 into the extracellular space. Lastly, treatment with recombinant p62 resulted in significantly increased expression of total AKT, as well as significantly increased expression of phosphorylated 4EBP1. These results align with the day 12 data obtained from *in vivo* IR injury and support the notion that UCHL1 regulates p62 expression and release, and that the extracellular p62 released by UCHL1 KD/smKO may affect intracellular mTOR pathway signaling.

In conclusion, this study built upon previous results and further characterized the role of UCHL1 in myogenesis. Aim 1 of this study provided evidence that UCHL1 is a negative regulator of muscle growth during development. Aim 2 of this study provided further evidence that UCHL1 negatively regulates myogenesis by partially inhibiting regeneration following injury. Furthermore, aim 2 provided evidence that UCHL1 also negatively regulates mTOR signaling activity, mitophagy related signaling activity, and that UCHL1 is potentially a positive mediator of macrophage recruitment and activation during the immune response. In addition, aim 3 of this study provided novel evidence that UCHL1

regulates directly interacts with p62, regulating expression and release through deubiquitinating function, although this does not directly regulate myogenesis. Aim 3 also showed that extracellular p62 upregulates intracellular DRP1 and mTOR signaling pathway activity. Overall, this study highlights UCHL1 as a potential therapeutic target for skeletal muscle injury, as well as a topic for further studies

CHAPTER 7

Limitations

Despite the clear evidence and novelty provided throughout this study, various limitations are still present. Although it is clear that UCHL1 is a negative regulator of myogenesis, this study was not able to identify the direct substrates responsible for improved myogenesis seen during development and regeneration in UCHL1 smKO mice. Moreover, other myogenic regulatory factors besides MyoD and myogenin could be affected by UCHL1 but were not assessed in this study. Aim 1 showed clear evidence that UCHL1 impacts muscle fiber type; however, this study was not able to identify the underlying mechanism behind this. Another limitation of this study arises from the H&E staining and immune response following injury. The lack of centrally located nuclei in injured muscle fibers suggests that they are not newly regenerated fibers, but rather that the muscle itself is more resistant to damage. The hematoxylin used to stain the nuclei was becoming old and less efficient, and thus it is possible that newer hematoxylin may have shown centrally located nuclei. On the other hand, if indeed the muscle is more resistant to damage which could be supported by the decreased immune response in UCHL1 smKO mice, further experiments are needed to confirm it and identify the responsible mechanism, or at least to identify where UCHL1 becomes involved during skeletal muscle injury. Aim 2 further identified a point of limitation regarding mitochondrial markers. While the upregulation of pink-1 and parkin by UCHL1 smKO strongly suggests enhanced mitophagy, more mitophagy markers and mechanisms should be further examined. Following this, the UCHL1-dependent regulation of P62 and its extracellular role suggests potential downstream affects related to increased regeneration following injury in UCHL1 smKO mice; however, the mechanism by which P62 indirectly contributes to myogenesis is still unclear. Lastly, though the evidence strongly suggests that UCHL1 regulates cellular function through the AKT-mTOR pathway, this study did not identify which signaling protein is directly associated with UCHL1, nor did it identify whether the upregulated AKT signaling activity was responsible for upregulated myogenesis or upregulated mitophagic activity, or both. It is clear that UCHL1 is a critical protein involved in multiple cellular functions within skeletal muscle, but further studies are needed to address the limitations of this study, and to further elucidate the role of UCHL1 in skeletal muscle development and regeneration.

CHAPTER 8

References

1. Day, I. N., & Thompson, R. J. (2010). UCHL1 (PGP 9.5): neuronal biomarker and ubiquitin system protein. *Progress in neurobiology*, *90*(3), 327-362.
2. Tramutola, A., Di Domenico, F., Barone, E., Perluigi, M., & Butterfield, D. A. (2016). It is all about (U) biquitin: role of altered ubiquitin-proteasome system and UCHL1 in Alzheimer disease. *Oxidative Medicine and Cellular Longevity*, *2016*.
3. Amerik, A. Y., & Hochstrasser, M. (2004). Mechanism and function of deubiquitinating enzymes. *Biochimica et Biophysica Acta (BBA)-Molecular Cell Research*, *1695*(1-3), 189-207.
4. Kim, J. H., Park, K. C., Chung, S. S., Bang, O., & Chung, C. H. (2003). Deubiquitinating enzymes as cellular regulators. *The journal of biochemistry*, *134*(1), 9-18.
5. Swatek, K. N., & Komander, D. (2016). Ubiquitin modifications. *Cell research*, *26*(4), 399-422.
6. Mi, Z., & Graham, S. H. (2023). Role of UCHL1 in the pathogenesis of neurodegenerative diseases and brain injury. *Ageing Research Reviews*, *86*, 101856.
7. Brackeva, B., De Punt, V., Kramer, G., Costa, O., Verhaeghen, K., Stangé, G., ... & Martens, G. A. (2015). Potential of UCHL1 as biomarker for destruction of pancreatic beta cells. Journal of proteomics, 117, 156-167.
8. Vasu, V. T., Ott, S., Hobson, B., Rashidi, V., Oommen, S., Cross, C. E., & Gohil, K. (2009). Sarcolipin and ubiquitin carboxy-terminal hydrolase 1 mRNAs are over-expressed in skeletal muscles of α-tocopherol deficient mice. Free radical research, 43(2), 106-116.
9. Powis, R. A., Mutsaers, C. A., Wishart, T. M., Hunter, G., Wirth, B., & Gillingwater, T. H. (2014). Increased levels of UCHL 1 are a compensatory response to disrupted ubiquitin homeostasis in spinal muscular atrophy and do not represent a viable therapeutic target. Neuropathology and applied neurobiology, 40(7), 873-887.
10. Gu, Y. Y., Yang, M., Zhao, M., Luo, Q., Yang, L., Peng, H., ... & Huang, C. Z. (2015). The de-ubiquitinase UCHL1 promotes gastric cancer metastasis via the Akt and Erk1/2 pathways. *Tumor Biology*, *36*, 8379-8387.

11. Kwan, S. Y., Au-Yeung, C. L., Yeung, T. L., Rynne-Vidal, A., Wong, K. K., Risinger, J. I., ... & Lu, K. H. (2020). Ubiquitin carboxyl-terminal hydrolase L1 (UCHL1) promotes uterine serous cancer cell proliferation and cell cycle progression. *Cancers*, *12*(1), 118.
12. Zhang, D., Fu, Y., Tian, G., Li, J., Shang, D., & Zhou, S. (2022). UCHL1 promotes proliferation and metastasis in head and neck squamous cell carcinoma and could be a potential therapeutic target. *Oral Surgery, Oral Medicine, Oral Pathology and Oral Radiology*, *133*(6), 684-697.
13. Jang, M. J., Baek, S. H., & Kim, J. H. (2011). UCH-L1 promotes cancer metastasis in prostate cancer cells through EMT induction. *Cancer letters*, *302*(2), 128-135.
14. Jin, C., Yu, W., Lou, X., Zhou, F., Han, X., Zhao, N., & Lin, B. (2013). UCHL1 is a putative tumor suppressor in ovarian cancer cells and contributes to cisplatin resistance. *Journal of Cancer*, *4*(8), 662.
15. Ummanni, R., Jost, E., Braig, M., Lohmann, F., Mundt, F., Barett, C., ... & Balabanov, S. (2011). Ubiquitin carboxyl-terminal hydrolase 1 (UCHL1) is a potential tumour suppressor in prostate cancer and is frequently silenced by promoter methylation. *Molecular cancer*, *10*, 1-13.
16. Xiang, T., Li, L., Yin, X., Yuan, C., Tan, C., Su, X., ... & Tao, Q. (2012). The ubiquitin peptidase UCHL1 induces G0/G1 cell cycle arrest and apoptosis through stabilizing p53 and is frequently silenced in breast cancer. *PloS one*, *7*(1), e29783.
17. Gao, H., Wu, P., Wang, X., & Li, Y. (2018). Deubiquitinase UCHL1 Regulates Myogenesis in Skeletal Muscles. *The FASEB Journal*, *32*, 769-6.
18. Li, Y., Gao, H., Wu, P., & Wang, X. (2018). UCHL1 regulates Interleukin-6 expression in skeletal muscles. *The FASEB Journal*, *32*, 907-11.
19. Gao, H., Freeling, J., Wu, P., Liang, A. P., Wang, X., & Li, Y. (2019). UCHL1 regulates muscle fibers and mTORC1 activity in skeletal muscle. *Life sciences*, *233*, 116699.
20. Gao, H., Antony, R., Srinivasan, R., Wu, P., Wang, X., & Li, Y. (2020). UCHL1 regulates oxidative activity in skeletal muscle. *PLoS One*, *15*(11), e0241716.
21. Gao, H., Hartnett, S., & Li, Y. (2017). Ubiquitin C-Terminal Hydrolase L1 regulates myoblast proliferation and differentiation. *Biochemical and biophysical research communications*, *492*(1), 96-102.

22. Frontera, W. R., & Ochala, J. (2015). Skeletal muscle: a brief review of structure and function. *Calcified tissue international*, *96*, 183-195.
23. Rose AJ, Richter EA. Skeletal muscle glucose uptake during exercise: how is it regulated? Physiology (Bethesda). 2005;20:260–70.
24. Richter EA, Hargreaves M. Exercise, GLUT4, and skeletal muscle glucose uptake. Physiol Rev. 2013;93(3):993–1017. pmid:23899560
25. Valentine, B. A. (2017). Skeletal muscle. *Pathologic basis of veterinary disease*, 908.
26. Morgan, J. E., & Partridge, T. A. (2003). Muscle satellite cells. *The international journal of biochemistry & cell biology*, *35*(8), 1151-1156.
27. Le Grand, F., & Rudnicki, M. A. (2007). Skeletal muscle satellite cells and adult myogenesis. *Current opinion in cell biology*, *19*(6), 628-633.
28. Scott, W., Stevens, J., & Binder–Macleod, S. A. (2001). Human skeletal muscle fiber type classifications. *Physical therapy*, *81*(11), 1810-1816.
29. Hopkins, P. M. (2006). Skeletal muscle physiology. *Continuing Education in Anaesthesia, Critical Care & Pain*, *6*(1), 1-6.
30. Kuo, I. Y., & Ehrlich, B. E. (2015). Signaling in muscle contraction. *Cold Spring Harbor perspectives in biology*, *7*(2), a006023.
31. Bentzinger, C. F., Wang, Y. X., & Rudnicki, M. A. (2012). Building muscle: molecular regulation of myogenesis. *Cold Spring Harbor perspectives in biology*, *4*(2), a008342.
32. Sabourin, L. A., & Rudnicki, M. A. (2000). The molecular regulation of myogenesis. *Clinical genetics*, *57*(1), 16-25.
33. Grefte, S., Kuijpers-Jagtman, A. M., Torensma, R., & Von den Hoff, J. W. (2007). Skeletal muscle development and regeneration. *Stem cells and development*, *16*(5), 857-868.
34. Buckingham, M., & Relaix, F. (2007). The role of Pax genes in the development of tissues and organs: Pax3 and Pax7 regulate muscle progenitor cell functions. *Annu. Rev. Cell Dev. Biol.*, *23*, 645-673.
35. Wang, J., & Conboy, I. (2010). Embryonic vs. adult myogenesis: challenging the ‘regeneration recapitulates development’paradigm. *Journal of molecular cell biology*, *2*(1), 1-4.

36. Hernández-Hernández, J. M., García-González, E. G., Brun, C. E., & Rudnicki, M. A. (2017, December). The myogenic regulatory factors, determinants of muscle development, cell identity and regeneration. In *Seminars in cell & developmental biology* (Vol. 72, pp. 10-18). Academic Press.
37. Asfour, H. A., Allouh, M. Z., & Said, R. S. (2018). Myogenic regulatory factors: The orchestrators of myogenesis after 30 years of discovery. *Experimental Biology and Medicine*, *243*(2), 118-128.
38. Baoge, L., Van Den Steen, E. L. K. E., Rimbaut, S., Philips, N., Witvrouw, E., Almqvist, K. F., ... & Vanden Bossche, L. C. (2012). Treatment of skeletal muscle injury: a review. *International Scholarly Research Notices*, *2012*.
39. Blaisdell, F. W. (2002). The pathophysiology of skeletal muscle ischemia and the reperfusion syndrome: a review. *Cardiovascular surgery*, *10*(6), 620-630.
40. Gillani, S., Cao, J., Suzuki, T., & Hak, D. J. (2012). The effect of ischemia reperfusion injury on skeletal muscle. *Injury*, *43*(6), 670-675.
41. Kalogeris, T., Baines, C. P., Krenz, M., & Korthuis, R. J. (2012). Cell biology of ischemia/reperfusion injury. *International review of cell and molecular biology*, *298*, 229-317.
42. Piper, H. M., Meuter, K., & Schäfer, C. (2003). Cellular mechanisms of ischemia-reperfusion injury. *The Annals of thoracic surgery*, *75*(2), S644-S648.
43. D'Oria M, Mani K, Rodriguez Lorenzo A. Microsurgical Salvage of Acute Lower Limb Ischemia after Iatrogenic Femoral Injury during Orthopedic Surgery in a Pediatric Patient. Ann Vasc Surg. 2020;69:452 e455-452 e411. doi: 10.1016/j.avsg.2020.06.064
44. Magan AA, Dunseath O, Armonis P, Fontalis A, Kayani B, Haddad FS. Tourniquet use in total knee arthroplasty and the risk of infection: a meta-analysis of randomised controlled trials. J Exp Orthop. 2022;9:62. doi: 10.1186/s40634-022-00485-9
45. Piper, H. M., Meuter, K., & Schäfer, C. (2003). Cellular mechanisms of ischemia-reperfusion injury. *The Annals of thoracic surgery*, *75*(2), S644-S648.
46. Eltzschig, H. K., & Eckle, T. (2011). Ischemia and reperfusion—from mechanism to translation. *Nature medicine*, *17*(11), 1391-1401.

47. Hausenloy, D. J., & Yellon, D. M. (2013). Myocardial ischemia-reperfusion injury: a neglected therapeutic target. *The Journal of clinical investigation*, *123*(1), 92-100.
48. Pantazi, E., Bejaoui, M., Folch-Puy, E., Adam, R., & Roselló-Catafau, J. (2016). Advances in treatment strategies for ischemia reperfusion injury. *Expert opinion on pharmacotherapy*, *17*(2), 169-179.
49. Malek, M., & Nematbakhsh, M. (2015). Renal ischemia/reperfusion injury; from pathophysiology to treatment. *Journal of renal injury prevention*, *4*(2), 20.
50. Lutz, J., Thürmel, K., & Heemann, U. (2010). Anti-inflammatory treatment strategies for ischemia/reperfusion injury in transplantation. *Journal of Inflammation*, *7*, 1-8.
51. Ahmed, A. U. (2011). An overview of inflammation: mechanism and consequences. *Frontiers in Biology*, *6*(4), 274-281.
52. Medzhitov, R. (2008). Origin and physiological roles of inflammation. *Nature*, *454*(7203), 428-435.
53. Antonelli, M., & Kushner, I. (2017). It's time to redefine inflammation. *The FASEB Journal*, *31*(5), 1787-1791.
54. Shen, H., Kreisel, D., & Goldstein, D. R. (2013). Processes of sterile inflammation. *The Journal of Immunology*, *191*(6), 2857-2863.
55. Rock, K. L., Latz, E., Ontiveros, F., & Kono, H. (2009). The sterile inflammatory response. *Annual review of immunology*, *28*, 321-342.
56. Costamagna, D., Costelli, P., Sampaolesi, M., & Penna, F. (2015). Role of inflammation in muscle homeostasis and myogenesis. *Mediators of inflammation*, *2015*.
57. Panci, G., & Chazaud, B. (2021, November). Inflammation during post-injury skeletal muscle regeneration. In *Seminars in Cell & Developmental Biology* (Vol. 119, pp. 32-38). Academic Press.
58. Arnold, L., Henry, A., Poron, F., Baba-Amer, Y., Van Rooijen, N., Plonquet, A., ... & Chazaud, B. (2007). Inflammatory monocytes recruited after skeletal muscle injury switch into antiinflammatory macrophages to support myogenesis. *The Journal of experimental medicine*, *204*(5), 1057-1069.

59. Howard, E. E., Pasiakos, S. M., Blesso, C. N., Fussell, M. A., & Rodriguez, N. R. (2020). Divergent roles of inflammation in skeletal muscle recovery from injury. *Frontiers in physiology*, *11*, 513331.
60. Qian, M., Fang, X., & Wang, X. (2017). Autophagy and inflammation. *Clinical and translational medicine*, *6*, 1-11.
61. Netea-Maier, R. T., Plantinga, T. S., van de Veerdonk, F. L., Smit, J. W., & Netea, M. G. (2016). Modulation of inflammation by autophagy: consequences for human disease. *Autophagy*, *12*(2), 245-260.
62. Matsuzawa-Ishimoto, Y., Hwang, S., & Cadwell, K. (2018). Autophagy and inflammation. *Annual review of immunology*, *36*, 73-101.
63. Mizushima, N. (2007). Autophagy: process and function. *Genes & development*, *21*(22), 2861-2873.
64. Kelekar, A. (2006). Autophagy. *Annals of the New York Academy of Sciences*, *1066*(1), 259-271.
65. Tanida, I. (2011). Autophagy basics. *Microbiology and immunology*, *55*(1), 1-11.
66. Glick, D., Barth, S., & Macleod, K. F. (2010). Autophagy: cellular and molecular mechanisms. *The Journal of pathology*, *221*(1), 3-12.
67. Sandri, M. (2010). Autophagy in skeletal muscle. *FEBS letters*, *584*(7), 1411-1416.
68. Xia, Q., Huang, X., Huang, J., Zheng, Y., March, M. E., Li, J., & Wei, Y. (2021). The role of autophagy in skeletal muscle diseases. *Frontiers in physiology*, *12*, 638983.
69. Stein, L. R., & Imai, S. I. (2012). The dynamic regulation of NAD metabolism in mitochondria. *Trends in Endocrinology & Metabolism*, *23*(9), 420-428.
70. Dölle, C., Rack, J. G., & Ziegler, M. (2013). NAD and ADP-ribose metabolism in mitochondria. *The FEBS journal*, *280*(15), 3530-3541.
71. Vakifahmetoglu-Norberg, H., Ouchida, A. T., & Norberg, E. (2017). The role of mitochondria in metabolism and cell death. *Biochemical and biophysical research communications*, *482*(3), 426-431.
72. Tzameli, I. (2012). The evolving role of mitochondria in metabolism. *Trends in Endocrinology & Metabolism*, *23*(9), 417-419.

73. Youle, R. J., & Narendra, D. P. (2011). Mechanisms of mitophagy. *Nature reviews Molecular cell biology*, *12*(1), 9-14.

74. Tolkovsky, A. M. (2009). Mitophagy. *Biochimica et Biophysica Acta (BBA)-Molecular Cell Research*, *1793*(9), 1508-1515.

75. Onishi, M., Yamano, K., Sato, M., Matsuda, N., & Okamoto, K. (2021). Molecular mechanisms and physiological functions of mitophagy. *The EMBO journal*, *40*(3), e104705.

76. Ding, W. X., & Yin, X. M. (2012). Mitophagy: mechanisms, pathophysiological roles, and analysis. *Biological chemistry*, *393*(7), 547-564.

77. Crawford, R. S., Hashmi, F. F., Jones, J. E., Albadawi, H., McCormack, M., Eberlin, K., ... & Watkins, M. T. (2007). A novel model of acute murine hindlimb ischemia. *American Journal of Physiology-Heart and Circulatory Physiology*, *292*(2), H830-H837.

78. Kim, J., Grotegut, C. A., Wisler, J. W., Mao, L., Rosenberg, P. B., Rockman, H. A., & Lefkowitz, R. J. (2020). The β-arrestin-biased β-adrenergic receptor blocker carvedilol enhances skeletal muscle contractility. *Proceedings of the National Academy of Sciences*, *117*(22), 12435-12443.

79. Li, J., Yang, Q., Han, L., Pan, C., Lei, C., Chen, H., & Lan, X. (2020). C2C12 mouse myoblasts damage induced by oxidative stress is alleviated by the antioxidant capacity of the active substance phloretin. *Frontiers in Cell and Developmental Biology*, *8*, 541260.

80. Weiss, A., & Leinwand, L. A. (1996). The mammalian myosin heavy chain gene family. *Annual review of cell and developmental biology*, *12*(1), 417-439.

81. Heissler, S. M., & Sellers, J. R. (2014). Myosin light chains: Teaching old dogs new tricks. *Bioarchitecture*, *4*(6), 169-188.

82. Hennig, P., Fenini, G., Di Filippo, M., Karakaya, T., & Beer, H. D. (2021). The pathways underlying the multiple roles of p62 in inflammation and cancer. *Biomedicines*, *9*(7), 707.

83. Yang, M., Linn, B. S., Zhang, Y., & Ren, J. (2019). Mitophagy and mitochondrial integrity in cardiac ischemia-reperfusion injury. *Biochimica et Biophysica Acta (BBA)-Molecular Basis of Disease*, *1865*(9), 2293-2302.

84. Pedersen, B. K., & Febbraio, M. A. (2012). Muscles, exercise and obesity: skeletal muscle as a secretory organ. *Nature Reviews Endocrinology*, *8*(8), 457-465.

85. Aoi, W. (2021). Myokines: A potential key factor in development, treatment, and biomarker of sarcopenia. In *Sarcopenia* (pp. 171-185). Elsevier.
86. Florin, A., Lambert, C., Sanchez, C., Zappia, J., Durieux, N., Tieppo, A. M., ... & Henrotin, Y. (2020). The secretome of skeletal muscle cells: A systematic review. *Osteoarthritis and Cartilage Open*, *2*(1), 100019.
87. Bjørkøy, G., Lamark, T., Pankiv, S., Øvervatn, A., Brech, A., & Johansen, T. (2009). Monitoring autophagic degradation of p62/SQSTM1. *Methods in enzymology*, *452*, 181-197.
88. Bjørkøy, G., Lamark, T., Brech, A., Outzen, H., Perander, M., Øvervatn, A., ... & Johansen, T. (2005). p62/SQSTM1 forms protein aggregates degraded by autophagy and has a protective effect on huntingtin-induced cell death. *The Journal of cell biology*, *171*(4), 603-614.
89. Kim, M. J., Deng, H. X., Wong, Y. C., Siddique, T., & Krainc, D. (2017). The Parkinson's disease-linked protein TMEM230 is required for Rab8a-mediated secretory vesicle trafficking and retromer trafficking. *Human molecular genetics*, *26*(4), 729-741.
90. Yu, X., Eischeid-Scholz, H., Meder, L., Kondylis, V., Büttner, R., & Odenthal, M. (2022). SQSTM1/p62 promotes miR-198 loading into extracellular vesicles and its autophagy-related secretion. *Human Cell*, *35*(6), 1766-1784.
91. Jo, Y. R., Oh, Y., Kim, Y. H., Shin, Y. K., Kim, H. R., Go, H., ... & Park, H. T. (2023). Adaptive autophagy reprogramming in Schwann cells during peripheral demyelination. *Cellular and Molecular Life Sciences*, *80*(1), 34.
92. Soutar, M. P., Kempthorne, L., Miyakawa, S., Annuario, E., Melandri, D., Harley, J., ... & Plun-Favreau, H. (2018). AKT signalling selectively regulates PINK1 mitophagy in SHSY5Y cells and human iPSC-derived neurons. *Scientific reports*, *8*(1), 8855.
93. Bishop, P., Rocca, D., & Henley, J. M. (2016). Ubiquitin C-terminal hydrolase L1 (UCH-L1): structure, distribution and roles in brain function and dysfunction. *Biochemical Journal*, *473*(16), 2453-2462.
94. Sanchez-Diaz, P. C., Chang, J. C., Moses, E. S., Dao, T., Chen, Y., & Hung, J. Y. (2017). Ubiquitin carboxyl-terminal esterase L1 (UCHL1) is associated with stem-like cancer cell functions in pediatric high-grade glioma. *PLoS One*, *12*(5), e0176879.

95. Jara, J. H., Frank, D. D., & Özdinler, P. H. (2013). Could dysregulation of UPS be a common underlying mechanism for cancer and neurodegeneration? Lessons from UCHL1. *Cell biochemistry and biophysics*, *67*, 45-53.

96. Xia, X., Xu, Q., Liu, M., Chen, X., Liu, X., He, J., ... & Liu, N. (2020). Deubiquitination of CD36 by UCHL1 promotes foam cell formation. *Cell Death & Disease*, *11*(8), 636.

97. Long, E. M., Long, M. A., Tsirigotis, M., & Gray, D. A. (2003). Stimulation of the murine Uchl1 gene promoter by the B-Myb transcription factor. *Lung Cancer*, *42*(1), 9-21.

98. Morkin, E. (1993). Regulation of myosin heavy chain genes in the heart. *Circulation*, *87*(5), 1451-1460.

99. Talmadge, R. J. (2000). Myosin heavy chain isoform expression following reduced neuromuscular activity: potential regulatory mechanisms. *Muscle & Nerve: Official Journal of the American Association of Electrodiagnostic Medicine*, *23*(5), 661-679.

100. Weiss, A., & Leinwand, L. A. (1996). The mammalian myosin heavy chain gene family. *Annual review of cell and developmental biology*, *12*(1), 417-439.

101. Tasić, D., Dimov, D., Gligorijević, J., Veličković, L., Katić, K., Krstić, M., & Dimov, I. (2003). Muscle fibre types and fibre morphometry in the tibialis posterior and anterior of the rat: a comparative study. *Facta universitatis-series: Medicine and Biology*, *10*(1), 16-21.

102. Chargé, S. B., & Rudnicki, M. A. (2004). Cellular and molecular regulation of muscle regeneration. *Physiological reviews*, *84*(1), 209-238.

103. Li, Y., il Lee, Y., & Thompson, W. J. (2011). Changes in aging mouse neuromuscular junctions are explained by degeneration and regeneration of muscle fiber segments at the synapse. *Journal of Neuroscience*, *31*(42), 14910-14919.

104. Carraro, U., Boncompagni, S., Gobbo, V., Rossini, K., Zampieri, S., Mosole, S., ... & Marcante, A. (2015). Persistent muscle fiber regeneration in long term denervation. past, present, future. *European journal of translational myology*, *25*(2).

105. Fukada, S. I., Higashimoto, T., & Kaneshige, A. (2022). Differences in muscle satellite cell dynamics during muscle hypertrophy and regeneration. *Skeletal muscle*, *12*(1), 17.

106. Zhou, L., Huang, H., McElfresh, T. A., Prosdocimo, D. A., & Stanley, W. C. (2008). Impact of anaerobic glycolysis and oxidative substrate selection on contractile function and mechanical efficiency during moderate severity ischemia. *American Journal of Physiology-Heart and Circulatory Physiology*, *295*(3), H939-H945.

107. Chatzinikita, E., Maridaki, M., Palikaras, K., Koutsilieris, M., & Philippou, A. (2023). The Role of Mitophagy in Skeletal Muscle Damage and Regeneration. *Cells*, *12*(5), 716.

108. Killackey, S. A., Philpott, D. J., & Girardin, S. E. (2020). Mitophagy pathways in health and disease. *Journal of Cell Biology*, *219*(11), e202004029.

109. Leduc-Gaudet, J. P., Hussain, S. N., Barreiro, E., & Gouspillou, G. (2021). Mitochondrial dynamics and mitophagy in skeletal muscle health and aging. *International Journal of Molecular Sciences*, *22*(15), 8179.

110. Flynn, J. M., & Melov, S. (2013). SOD2 in mitochondrial dysfunction and neurodegeneration. *Free Radical Biology and Medicine*, *62*, 4-12.

111. Deng, B., Wehling-Henricks, M., Villalta, S. A., Wang, Y., & Tidball, J. G. (2012). IL-10 triggers changes in macrophage phenotype that promote muscle growth and regeneration. *The Journal of Immunology*, *189*(7), 3669-3680.

112. Arnold, L., Henry, A., Poron, F., Baba-Amer, Y., Van Rooijen, N., Plonquet, A., ... & Chazaud, B. (2007). Inflammatory monocytes recruited after skeletal muscle injury switch into antiinflammatory macrophages to support myogenesis. *The Journal of experimental medicine*, *204*(5), 1057-1069.

113. Juban, G. (2021, November). Transcriptional control of macrophage inflammatory shift during skeletal muscle regeneration. In *Seminars in Cell & Developmental Biology* (Vol. 119, pp. 82-88). Academic Press.

114. Wang, H., Melton, D. W., Porter, L., Sarwar, Z. U., McManus, L. M., & Shireman, P. K. (2014). Altered macrophage phenotype transition impairs skeletal muscle regeneration. *The American journal of pathology*, *184*(4), 1167-1184.

115. Saclier, M., Cuvellier, S., Magnan, M., Mounier, R., & Chazaud, B. (2013). Monocyte/macrophage interactions with myogenic precursor cells during skeletal muscle regeneration. *The FEBS journal*, *280*(17), 4118-4130.

116. William, M., Leroux, L. P., Chaparro, V., Lorent, J., Graber, T. E., M'Boutchou, M. N., ... & Jaramillo, M. (2018). eIF4E-binding proteins 1 and 2 limit macrophage anti-inflammatory responses through translational repression of IL-10 and cyclooxygenase-2. *The Journal of Immunology*, *200*(12), 4102-4116.

117. William, M., Leroux, L. P., Chaparro, V., Graber, T. E., Alain, T., & Jaramillo, M. (2019). Translational repression of Ccl5 and Cxcl10 by 4E-BP1 and 4E-BP2 restrains the ability of mouse macrophages to induce migration of activated T cells. *European Journal of Immunology*, *49*(8), 1200-1212.

118. Pearl, D., Katsumura, S., Amiri, M., Tabatabaei, N., Zhang, X., Vinette, V., ... & Tahmasebi, S. (2020). 4E-BP–Dependent Translational Control of Irf8 Mediates Adipose Tissue Macrophage Inflammatory Response. *The Journal of Immunology*, *204*(9), 2392-2400.

119. Yang, H., Ye, X., Zhang, X., Li, X., Fu, Q., & Tang, Z. (2018). Intracellular osteopontin negatively regulates toll-like receptor 4-mediated inflammatory response via regulating GSK3β and 4EBP1 phosphorylation. *Cytokine*, *108*, 89-95.

120. Grolleau, A., Sonenberg, N., Wietzerbin, J., & Beretta, L. (1999). Differential regulation of 4E-BP1 and 4E-BP2, two repressors of translation initiation, during human myeloid cell differentiation. *The Journal of Immunology*, *162*(6), 3491-3497.

121. McFarland HI, Nahill SR, Maciaszek JW, Welsh RM. CD11b (Mac-1): a marker for CD8+ cytotoxic T cell activation and memory in virus infection. J Immunol. 1992 Aug 15;149(4):1326-33. PMID: 1500720.

122. Zhang, Z., Liu, N., Chen, X., Zhang, F., Kong, T., Tang, X., ... & Chen, X. (2021). UCHL1 regulates inflammation via MAPK and NF-κB pathways in LPS-activated macrophages. *Cell Biology International*, *45*(10), 2107-2117.

123. Huang, Y., He, S., Chen, Y., Sheng, J., Fu, Y., Du, X., ... & Ma, L. (2022). UCHL1 promoted polarization of M1 macrophages by regulating the PI3K/AKT signaling pathway. *Journal of Inflammation Research*, 735-746.

124. Hennig, P., Fenini, G., Di Filippo, M., Karakaya, T., & Beer, H. D. (2021). The pathways underlying the multiple roles of p62 in inflammation and cancer. *Biomedicines*, *9*(7), 707.

125. Valencia, T., Kim, J. Y., Abu-Baker, S., Moscat-Pardos, J., Ahn, C. S., Reina-Campos, M., ... & Moscat, J. (2014). Metabolic reprogramming of stromal fibroblasts through p62-mTORC1 signaling promotes inflammation and tumorigenesis. *Cancer cell*, *26*(1), 121-135.

126. Lee, H. M., Shin, D. M., Yuk, J. M., Shi, G., Choi, D. K., Lee, S. H., ... & Jo, E. K. (2011). Autophagy negatively regulates keratinocyte inflammatory responses via scaffolding protein p62/SQSTM1. *The Journal of Immunology*, *186*(2), 1248-1258.

127. Yang, S., Li, F., Lu, S., Ren, L., Bian, S., Liu, M., ... & Wang, J. (2022). Ginseng root extract attenuates inflammation by inhibiting the MAPK/NF-κB signaling pathway and activating autophagy and p62-Nrf2-Keap1 signaling in vitro and in vivo. *Journal of Ethnopharmacology*, *283*, 114739.

128. Ishii, T., Warabi, E., Siow, R. C., & Mann, G. E. (2013). Sequestosome1/p62: a regulator of redox-sensitive voltage-activated potassium channels, arterial remodeling, inflammation, and neurite outgrowth. *Free Radical Biology and Medicine*, *65*, 102-116.

129. Zhong, J., Zhao, M., Ma, Y., Luo, Q., Liu, J., Wang, J., ... & Huang, C. (2012). UCHL1 acts as a colorectal cancer oncogene via activation of the β-catenin/TCF pathway through its deubiquitinating activity. *International journal of molecular medicine*, *30*(2), 430-436.

130. Ha, J., Kim, M., Seo, D., Park, J. S., Lee, J., Lee, J., & Park, S. H. (2020). The deubiquitinating enzyme USP20 regulates the TNFα-induced NF-κB signaling pathway through stabilization of p62. *International Journal of Molecular Sciences*, *21*(9), 3116.

131. Lee, B., Kim, Y. H., Lee, W., Choi, H. Y., Lee, J., Kim, J., ... & Shin, J. S. (2023). USP13 deubiquitinates p62/SQSTM1 to induce autophagy and Nrf2 release for activating antioxidant response genes. *Free Radical Biology and Medicine*, *208*, 820-832.

132. Peng, H., Yang, F., Hu, Q., Sun, J., Peng, C., Zhao, Y., & Huang, C. (2020). The ubiquitin-specific protease USP8 directly deubiquitinates SQSTM1/p62 to suppress its autophagic activity. *Autophagy*, *16*(4), 698-708.

133. Clausen, L., Abildgaard, A. B., Gersing, S. K., Stein, A., Lindorff-Larsen, K., & Hartmann-Petersen, R. (2019). Protein stability and degradation in health and disease. *Advances in protein chemistry and structural biology*, *114*, 61-83.

134. Potes, Y., Bermejo-Millo, J. C., Mendes, C., Castelão-Baptista, J. P., Díaz-Luis, A., Pérez-Martínez, Z., ... & Vega-Naredo, I. (2024). p66Shc signaling and autophagy impact on C2C12 myoblast differentiation during senescence. *Cell Death & Disease*, *15*(3), 200.

135. Jiang, A., Guo, H., Wu, W., & Liu, H. (2021). The crosstalk between autophagy and apoptosis is necessary for myogenic differentiation. *Journal of Agricultural and Food Chemistry*, *69*(13), 3942-3951.

136. Zhou, Y., Hua, S., & Song, L. (2023). The versatile defender: exploring the multifaceted role of p62 in intracellular bacterial infection. *Frontiers in Cellular and Infection Microbiology*, *13*, 1180708.

137. Hennig, P., Fenini, G., Di Filippo, M., Karakaya, T., & Beer, H. D. (2021). The pathways underlying the multiple roles of p62 in inflammation and cancer. *Biomedicines*, *9*(7), 707.

138. Snyder, N. A., & Silva, G. M. (2021). Deubiquitinating enzymes (DUBs): Regulation, homeostasis, and oxidative stress response. *Journal of Biological Chemistry*, *297*(3).

139. Snyder, N. A., & Silva, G. M. (2021). Deubiquitinating enzymes (DUBs): Regulation, homeostasis, and oxidative stress response. *Journal of Biological Chemistry*, *297*(3).

140. Harris, I. S., Endress, J. E., Coloff, J. L., Selfors, L. M., McBrayer, S. K., Rosenbluth, J. M., ... & Brugge, J. S. (2019). Deubiquitinases maintain protein homeostasis and survival of cancer cells upon glutathione depletion. *Cell metabolism*, *29*(5), 1166-1181.

141. von Maltzahn, J., Chang, N. C., Bentzinger, C. F., & Rudnicki, M. A. (2012). Wnt signaling in myogenesis. *Trends in cell biology*, *22*(11), 602-609.

142. Cossu, G., & Borello, U. (1999). Wnt signaling and the activation of myogenesis in mammals. *The EMBO journal*, *18*(24), 6867-6872.

143. Girardi, F., & Le Grand, F. (2018). Wnt signaling in skeletal muscle development and regeneration. *Progress in molecular biology and translational science*, *153*, 157-179.

144. Brack, A. S., Conboy, I. M., Conboy, M. J., Shen, J., & Rando, T. A. (2008). A temporal switch from notch to Wnt signaling in muscle stem cells is necessary for normal adult myogenesis. *Cell stem cell*, *2*(1), 50-59.

145. Jara, J. H., Frank, D. D., & Özdinler, P. H. (2013). Could dysregulation of UPS be a common underlying mechanism for cancer and neurodegeneration? Lessons from UCHL1. *Cell biochemistry and biophysics*, *67*, 45-53.

146. Zhong, J., Zhao, M., Ma, Y., Luo, Q., Liu, J., Wang, J., ... & Huang, C. (2012). UCHL1 acts as a colorectal cancer oncogene via activation of the β-catenin/TCF pathway through its deubiquitinating activity. *International journal of molecular medicine*, *30*(2), 430-436.

147. Zhang, H., Luo, W., Sun, Y., Qiao, Y., Zhang, L., Zhao, Z., & Lv, S. (2016). Wnt/β-catenin signaling mediated-UCH-L1 expression in podocytes of diabetic nephropathy. *International Journal of Molecular Sciences*, *17*(9), 1404.

148. Xing, M., Li, P., Wang, X., Li, J., Shi, J., Qin, J., ... & Zhang, J. Y. (2019). Overexpression of p62/IMP2 can promote cell migration in hepatocellular carcinoma via activation of the Wnt/β-catenin pathway. *Cancers*, *12*(1), 7.

149. Lorzadeh, S., Kohan, L., Ghavami, S., & Azarpira, N. (2021). Autophagy and the Wnt signaling pathway: A focus on Wnt/β-catenin signaling. *Biochimica et Biophysica Acta (BBA)-Molecular Cell Research*, *1868*(3), 118926.

150. Lorzadeh, S., Kohan, L., Ghavami, S., & Azarpira, N. (2021). Autophagy and the Wnt signaling pathway: A focus on Wnt/β-catenin signaling. *Biochimica et Biophysica Acta (BBA)-Molecular Cell Research*, *1868*(3), 118926.

151. Colella, B., Faienza, F., Carinci, M., D'Alessandro, G., Catalano, M., Santoro, A., ... & Di Bartolomeo, S. (2019). Autophagy induction impairs Wnt/β-catenin signalling through β-catenin relocalisation in glioblastoma cells. *Cellular signalling*, *53*, 357-364.

152. Oh, W. J., & Jacinto, E. (2011). mTOR complex 2 signaling and functions. *Cell cycle*, *10*(14), 2305-2316.